# การรีฟอร์มมิงด้วยคาร์บอนไดออกไซด์และการออกซิเดชันบางส่วนที่ส่งเสริมด้วยการดูดซับของก๊าซชีวภาพ

นางสาวพรนิภา  สนธิสง่า

วิทยานิพนธ์นี้เป็นส่วนหนึ่งของการศึกษาตามหลักสูตรปริญญาวิศวกรรมศาสตรมหาบัณฑิต
สาขาวิชาวิศวกรรมเคมี ภาควิชาวิศวกรรมเคมี
คณะวิศวกรรมศาสตร์ จุฬาลงกรณ์มหาวิทยาลัย
ปีการศึกษา 2551

# SORPTION-ENHANCED CARBON DIOXIDE REFORMING AND PARTIAL OXIDATION OF BIOGAS

Miss Pornnipa Sonthisanga

A Thesis Submitted in Partial Fulfillment of the Requirements
for the Degree of Master of Engineering Program in Chemical Engineering
Department of Chemical Engineering
Faculty of Engineering
Chulalongkorn University
Academic Year 2008

| | |
|---|---|
| Thesis Title | SORPTION-ENHANCED CARBON DIOXIDE REFORMING AND PARTIAL OXIDATION OF BIOGAS |
| By | Miss Pornnipa Sonthisanga |
| Field of Study | Chemical Engineering |
| Thesis Advisor | Professor Suttichai Assabumrungrat, Ph.D. |

---

Accepted by the Faculty of Engineering, Chulalongkorn University in Partial Fulfillment of the Requirements for the Master's Degree

........................................................ Dean of the Faculty of Engineering

(Associate Professor Boonsom Lerdhirunwong, Dr.Ing.)

THESIS COMMITTEE

Montree Wongsri ........................................ Chairman

(Assistant Professor Montree Wongsri, D.Sc.)

........................................................ Advisor

(Professor Suttichai Assabumrungrat, Ph.D.)

... .................................................... Co-Advisor

(Assistant Professor Navadol Laosiripojana, Ph.D.)

........................................................ Examiner

(Assistant Professor Bunjerd Jongsomjit, Ph.D.)

........................................................ External Examiner

(Assistant Professor Worapon Kiatkittipong, D.Eng.)

พรนิภา สนธิสง่า: การรีฟอร์มมิงด้วยคาร์บอนไดออกไซด์และการออกซิเดชันบางส่วนที่ส่งเสริมด้วยการดูดซับของก๊าซชีวภาพ (SORPTION-ENHANCED CARBON DIOXIDE REFORMING AND PARTIAL OXIDATION OF BIOGAS) อ.ที่ปรึกษาวิทยานิพนธ์หลัก: ศ.ดร. สุทธิชัย อัสสะบำรุงรัตน์, อ.ที่ปรึกษาวิทยานิพนธ์ร่วม: ผศ.ดร. นวดล เหล่าศิริพจน์, 68 หน้า

งานวิจัยนี้ทำการศึกษาประโยชน์ของการใช้แคลเซียมออกไซด์เป็นตัวดูดซับคาร์บอนไดออกไซด์ในปฏิกิริยารีฟอร์มมิงด้วยคาร์บอนไดออกไซด์และการออกซิเดชันบางส่วนของก๊าซชีวภาพโดยใช้ตัวเร่งปฏิกิริยาโลหะนิกเกิลบนตัวรองรับซิลิกอนไดออกไซด์และแมกนีเซียมออกไซด์ สมรรถนะทางปฏิกิริยาเคมีในรูปผลได้ไฮโดรเจนของระบบปฏิกิริยาที่ร่วมกับการดูดซับภายใต้ 3 แบบ 1) ตัวเร่งปฏิกิริยาก่อนแคลเซียมออกไซด์ 2) แคลเซียมออกไซด์ก่อนตัวเร่งปฏิกิริยา 3) การผสมแคลเซียมออกไซด์และตัวเร่งปฏิกิริยา ซึ่งเปรียบเทียบกับระบบทั่วไปปราศจากแคลเซียมออกไซด์ จากผลบ่งชี้ว่าระบบของการผสมแคลเซียมออกไซด์และตัวเร่งปฏิกิริยาแสดงสมรรถนะดีที่สุดท่ามกลางระบบส่งเสริมด้วยการดูดซับแบบอื่น อย่างไรก็ตามผลจากกระบวนการจำลองบ่งชี้ว่าการเติมออกซิเจนส่งผลให้สัดส่วนไฮโดรเจนต่อคาร์บอนมอนอกไซด์ ร้อยละผลได้ไฮโดรเจนและความเข้มข้นไฮโดรเจนลดลงแต่ความร้อนที่ได้จากปฏิกิริยาคายความร้อนเพิ่มขึ้น การเติมน้ำสามารถส่งเสริมสัดส่วนไฮโดรเจนต่อคาร์บอนมอนอกไซด์ ร้อยละผลได้ไฮโดรเจนและความร้อนที่ได้จากปฏิกิริยาดูดความร้อนยกเว้นความเข้มข้นไฮโดรเจนลดลง การเติมแคลเซียมออกไซด์สามารถปรับปรุงสัดส่วนไฮโดรเจนต่อคาร์บอนมอนอกไซด์ ร้อยละผลได้ไฮโดรเจนความเข้มข้นไฮโดรเจนรวมถึงความร้อนที่ได้จากปฏิกิริยาคายความร้อนให้ดีขึ้น ผลของอุณหภูมิสัดส่วนไฮโดรเจนต่อคาร์บอนมอนอกไซด์ ร้อยละผลได้ไฮโดรเจนและความเข้มข้นไฮโดรเจนลดลงแต่เอนทัลปีรวมเพิ่มขึ้นที่อุณหภูมิสูง สำหรับระบบเทอร์มอล-นิวทรอล สภาวะที่ให้ร้อยละผลได้ไฮโดรเจนมากที่สุด (89.3%) และสัดส่วนไฮโดรเจนต่อคาร์บอนมอนอกไซด์เท่ากับ 8.98 คือสัดส่วนออกซิเจนต่อมีเทนเท่ากับ 0.00013 สัดส่วนน้ำต่อมีเทนเท่ากับ 4.8 และสัดส่วนแคลเซียมออกไซด์ต่อมีเทนเท่ากับ 1 ที่อุณหภูมิ 973 เคลวิน

ภาควิชา วิศวกรรมเคมี
สาขาวิชา วิศวกรรมเคมี
ปีการศึกษา 2551

ลายมือชื่อนิสิต พรนิภา สนธิสง่า
ลายมือชื่อ อ.ที่ปรึกษาวิทยานิพนธ์หลัก
ลายมือชื่อ อ.ที่ปรึกษาวิทยานิพนธ์ร่วม

# # 5070365021: MAJOR CHEMICAL ENGINEERING

KEYWORDS: CARBON DIOXIDE REFORMING / PARTIAL OXIDATION / SORPTION / THERMAL-NEUTRAL OPERATION.

PORNNIPA SONTHISANGA: SORPTION-ENHANCED CARBON DIOXIDE REFORMING AND PARTIAL OXIDATION OF BIOGAS. ADVISOR: SUTTICHAI ASSABUMRUNGRAT, Ph.D., CO-ADVISOR: NAVADOL LAOSIRIPOJANA, Ph.D., 68 pp.

This work investigates the advantages of utilizing CaO as a $CO_2$ sorbent in the combined carbon dioxide reforming and partial oxidation of biogas over $Ni/SiO_2.MgO$ catalyst. The catalytic performance in term of hydrogen yield of the integrated sorption-reaction systems was operated under 3 modes; i.e. i) $Ni/SiO_2.MgO$ before CaO, ii) CaO before $Ni/SiO_2.MgO$ and iii) mixture of CaO and $Ni/SiO_2.MgO$, is compared with that of the conventional system without CaO sorbent. The results indicate that the mode of mixture of CaO and $Ni/SiO_2.MgO$ shows the best performance among the different sorption enhanced systems. However, the results from simulation indicated that the addition of oxygen caused decrease in $H_2$:CO ratio, hydrogen yield and concentration, but increase in exothermic heat. The addition of water was able to enhance $H_2$:CO ratio, hydrogen yield and endothermic heat; however, hydrogen concentration was declined. The CaO addition can improve $H_2$:CO ratio, hydrogen yield and concentration including more exothermic heat. The temperature effect, $H_2$: CO ratio, hydrogen yield and concentration decreased but the overall enthalpy increased at high temperature. For thermal-neutral operation, the condition which gives optimum hydrogen yield of 89.3% with $H_2:CO = 8.98$ are $O_2:CH_4 = 0.00013$, $H_2O:CH_4 = 4.8$ and $CaO:CH_4 = 1$ at 973 K.

Department :....Chemical Engineering...
Field of Study :...Chemical Engineering.
Academic Year :......2008................

Student's Signature ...Pornnipa Sonthisanga
Advisor's Signature ...........................
Co-Advisor's Signature..........

# ACKNOWLEDGEMENTS

The author would like to express her greatest gratitude and appreciation to Professor Dr. Suttichai Assabumrungrat, her advisor, for her invaluable suggestions, encouragement during her study and useful discussions throughout this research. Her advice is always worthwhile and without her this work could not be possible.

The author wishes to thank Assistant Professor Dr. Montree Wongsri, as the chairman, Assistant Professor Navadol Laosiripojana, Assistant Professor Worapon Kiatkittipong and Assistant Professor Dr. Bunjerd Jongsomjit as the members of the thesis committee for their valuable guidance and revision throughout her thesis.

The financial supports of the Graduate School of Chulalongkorn University and Department of Chemical Engineering are gratefully acknowledged. Most of all, the author would like to express her highest gratitude to her parents who always take care and encourage her. The most success of graduation is devoted to her parents.

Finally, the author wishes to thank Dr. Pakorn Piroonlerkgul and the members of the Center of Excellence on Catalysis and Catalytic Reaction Engineering, Department of Chemical Engineering, Faculty of Engineering, Chulalongkorn University for friendship. To many others, not specifically named, who have provided her with support and encouragement, please be assured that she thinks of you.

# CONTENTS

Page

# LIST OF TABLES

**Table** **Page**

# LIST OF FIGURES

**Figure** **page**

**Figure** **page**

**Figure** **page**

# CHAPTER I

# INTRODUCTION

## 1.1 Introduction

Syngas or synthesis gas is the name given to a gas mixture that contains varying amounts of carbon monoxide and hydrogen. The name comes from its use as an intermediate in creating synthetic natural gas (SNG), ammonia or methanol. It is also used in production of synthetic petroleum for use as a fuel or lubricant via Fischer-Tropsch synthesis and previously the Mobil methanol to gasoline process. The production of synthesis gas from hydrocarbons can be achieved via different processes such as steam reforming, partial oxidation, carbon dioxide reforming (or dry reforming) and autothermal reforming, offering different ratios of hydrogen to carbon monoxide. When hydrogen is the desired product, carbon monoxide can be further converted to hydrogen via water gas shift reaction.

Synthesis gas is industrially produced through the steam reforming of methane. However, the steam reforming of methane requires temperatures above 1000 K, as well as a large energy input due to a highly endothermic reaction. Thus, the production of synthesis gas through the partial oxidation of methane is of a current interest, because the reaction is an exothermic one. The partial oxidation of methane produces synthesis gas of $H_2$/CO ratio = 2, whereas the $H_2$/CO ratio for the steam reforming of methane is 3. The $H_2$/CO ratio equal to 2 is suitable for the synthesis of methanol and higher hydrocarbons (Takenaka et al., 2007). In addition, the rate of the partial oxidation of methane is also much faster than that of the steam reforming of methane, suggesting that a single-stage process for synthesis gas production would be more attractive than the steam reforming of methane and would also result in smaller reactors and higher productivity (Li and Lu, 2004).

For carbon dioxide reforming process, synthesis gas produced is in a low $H_2$/CO ratio which is useful for the synthesis of hydroformylation and carbonylation reactions as well as for methanol, oxygenated compounds and Fischer–Tropsch syntheses. Furthermore, carbon dioxide reforming of methane is an efficient process for producing CO rich synthesis gas with additional advantage on environmental view point as both methane and carbon dioxide are major greenhouse gases contributing to global warming or “Greenhouse Effect”. The effect of global warming has been linked to increased height of sea levels at coastal areas, melting of glaciers, and climatic change in ecosystem (Khatri, 2005).

In the previous studies of our group, the carbon dioxide reforming of methane was investigated (Promaros et al., 2005). The reaction was carried out under the periodic operation mode in which the feed is alternately switched between methane and carbon dioxide. Under methane feed, hydrogen is generated and exits the catalyst bed, leaving carbon depositing on the catalyst. Then carbon dioxide reacts with the deposited carbon, forming carbon monoxide as the product. This operation is beneficial particularly when pure hydrogen is desired. From our study, it was reported that the performance of periodic operation for the carbon dioxide reforming of methane over an industrial steam reforming $Ni/SiO_2.MgO$ catalyst was lower than that of the steady-state operation over all ranges of reaction time for both reaction temperatures of 923 and 1023 K. Because deposited carbon was incompletely removed by carbon dioxide in the regeneration step. Therefore, the efficient process for carbon removal by oxygen addition is required to improve the catalytic activity and stability in the next study (Charoenseri, 2007). The addition of oxygen into the carbon dioxide reforming of methane at 1023 K was able to improve the catalytic stability in terms of methane conversion. The periodic operation offered the hydrogen yield close to that of the steady state operation at 923 K. The lower amount of coke was formed on the catalyst surface after exposure to the combined reactions at higher oxygen content and reaction temperature for both periodic and steady state operations.

At present, the researches on hydrogen production are numerous as hydrogen is considered to be a potential clean fuel for future. Various fuels such as methane, methanol, ethanol and gasoline can be used as the feedstock for hydrogen production. Biogas is considered as an attractive green fuel because it can be produced by anaerobic digestion or fermentation of biodegradable materials such as biomass, manure or sewage, municipal waste, green waste and energy crops. It has been used as a low-cost fuel in many countries for any heating purpose, such as cooking and also used in modern waste management facilities for running any type of heat engine, generating either mechanical or electrical power. According to the global warming problem, it is desired to reduce the carbon dioxide emission to the environment. Therefore, a CaO sorption process, a well-known carbon dioxide capture technology nowadays, has been integrated with some hydrogen-generating reactions to remove carbon dioxide for further sequestration and in some cases can further enhance the operation, for example, exothermic heat arisen from carbon dioxide sorption can be utilized for the reactions.

In this work, the sorption-enhanced operation of combined carbon dioxide reforming and partial oxidation of biogas is investigated. In the experimental study, biogas and oxygen are simultaneously introduced to a reactor packed with a mixture of industrial steam reforming $Ni/SiO_2.MgO$ catalyst and CaO adsorbent. Excess carbon dioxide is adsorbed on CaO not to emit carbon dioxide. Therefore, the main product is synthesis gas. The effect of adsorbent and catalyst bed arrangement; i) CaO before $Ni/SiO_2.MgO$, ii) mixture of CaO and $Ni/SiO_2.MgO$ and iii) $Ni/SiO_2.MgO$ before CaO is investigated. The thermal-neutral process, combined adsorption of CaO with reactions of biogas, is investigated. Finally, the operating conditions which offer thermal-neutral operation using Aspen Plus Simulator are determined.

## 1.2 Objective

To study a combined system of carbon dioxide reforming, partial oxidation and $CO_2$ adsorption for synthesis gas/hydrogen production from biogas, to investigate effects of operating parameters (i.e., $O_2/CH_4$ and $CaO/CH_4$ ratios, operating temperature and $H_2O/CH_4$ ratio) on the system performance ($H_2$ yield, $H_2$ concentration, $CO/H_2$ ratio and reaction heat) and to determine operating condition which offers thermal-neutral operation.

## 1.3 Thesis Organization

This thesis is organized as follows:

Chapter I is the general introduction addressing the rationale and objective of this work.

Chapter II reviews research work on sorption-enhanced reaction process, combined carbon dioxide reforming and partial oxidation of methane and catalytic cracking of methane and catalyst regeneration reaction in the past.

Chapter III provides the fundamental theory for this work, i.e. the reactions for synthesis gas production and sorption enhanced reaction process.

The experimental as well as chemicals and materials, apparatus and experimental procedures used for studying reaction in this work are presented in Chapter IV.

The experimental results and discussion are described in Chapter V.

The overall conclusion drawn from this work and some recommendations for future research work are provided in Chapter VI

Finally, the sample of calculation for conversion, calibration curves from area to mole of product, and reactant gases, and the experimental data are included in appendices at the end of this thesis.

# CHAPTER II

# LITERATURE REVIEWS

The literature review is divided into two main parts. The first part is research and development on sorption-enhanced reaction process. The second part reviews combined carbon dioxide reforming and partial oxidation of methane.

## 2.1 Sorption-enhanced reaction process

Sorption-enhanced reaction process is a fixed bed process with the reactor containing a mixture of a conventional catalyst and a high temperature adsorbent that selectively removes one or more of the products produced during the catalytic reaction. For an equilibrium limited reaction, the adsorbent shifts the equilibrium in favor of increased conversion through Le Chatlier's principal.

The adsorbent used in this work is CaO. This adsorbent was investigated by Han and Harrison (1994), Abanades, J. C. (2002), Gupta et al. (2002) and Dasgupta et al. (2008). This material also showed high $CO_2$ capacity at high temperature with reasonable regeneration rate.

Barelli et al. (2008) reviewed the steam methane reforming (SMR) process and methodologies for performances improvement. The focus was on the sorption-enhanced steam methane reforming (SE-SMR) process in which sorbents are added in order to enhance the reactions and realize in-situ $CO_2$ separation. Hydrogen production can also be improved by selective permeation through a membrane, or selective permeation through simultaneous reaction of the targeted molecule. In particular, significant improvements were realized in the case of addition of a $CO_2$ acceptor to the reactor. In such case, in fact, carbon dioxide is converted to a solid carbonate as soon as it is formed, shifting the reversible reforming and water-gas shift reaction beyond their conventional thermodynamic limits, while the regeneration of the sorbent releases a mixture of relatively pure $CO_2$ and inert gas.

The advantages of combining steam reforming with in-situ $CO_2$ capture can be seen in thermodynamic point of views. The equilibrium hydrogen concentration as a function of reaction temperature at ambient pressure and with a S/C equal to 3 is shown in Fig.2.1. Sorption enhancement enables both lower reaction temperatures, which may reduce catalyst coking and sintering, and the consequent use of less expensive reactor wall materials. In addition, heat released by the exothermic carbonation reaction supplies most of the heat required by the endothermic reforming reactions.

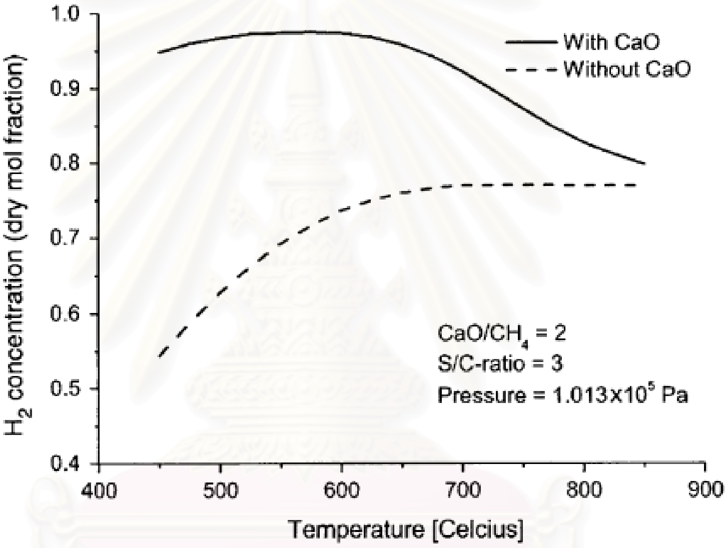

**Fig. 2.1** Hydrogen content at equilibrium as a function of temperature for a pressure of $1.013 \times 10^5$ Pa, a $H_2O:CH_4$ molar ratio of 3 and a $CaO:CH_4$ molar ratio of 2. (Barelli et al., 2008)

Sorption-enhanced steam reforming and the use of calcium based $CO_2$ sorbents has been studied by several researchers. For example, Balasubramanian et al. (1999) investigated production of hydrogen from methane in a single-step process. They added a calcium-based $CO_2$ acceptor to a commercial steam reforming catalyst producing more 95% hydrogen concentration in a laboratory-scale fixed bed reactor. Han and Harrison (1994) investigated simultaneous the water-gas shift reaction and carbon dioxide separation for the direct production of hydrogen. They used CaO sorbent to capture $CO_2$ in a tubular reactor, overcoming the equilibrium limitation and achieving complete CO conversion.

Sorption-enhanced steam reforming of methane in a fluidized bed reactor over a mixture of commercial Ni-based steam reforming catalyst and dolomite as $CO_2$-acceptor which captured $CO_2$ in order to shift the steam reforming equilibrium for the production of hydrogen was studied by Johnsen et al. (2006). They found that equilibrium hydrogen concentration more 98% on a dry basis was reached at 873 K and 1 atm, with dolomite as the $CO_2$-acceptor. The hydrogen concentration remained at 98–99 % (dry basis) after four reforming/calcination cycles. The total production time decreased with an increasing number of cycles due to loss of $CO_2$-uptake capacity of the dolomite, but the reaction rate seemed unaffected. Variation of the superficial gas velocity within the bubbling bed regime showed that the overall reaction rate was sufficiently fast to reach equilibrium, making bubbling bed reactors attractive for this process.

Halmann and Steinfeld (2006) investigated thermal-neutral process by combining the $CO_2$-releasing calcination of $CaCO_3$ with the $CO_2$-consuming dry-reforming of methane, and by further combining these endothermic reactions with the exothermic partial oxidation of methane. A single thermal-neutral process can be designed for co-producing CaO and synthesis gas in an autothermal reactor. Synthesis gas can be further processed to hydrogen, methanol, or Fischer–Tropsch chemicals. The conditions for thermo-neutrality are determined by thermo chemical equilibrium calculations. Such combined processes could achieve considerable $CO_2$ emission avoidance as well as fuel saving relative to the conventional production of CaO and synthesis gas. The preliminary evaluations indicate that the thermo-neutral co-production of CaO and hydrogen or methanol from $CaCO_3$+ $O_2$+$H_2O$ and natural gas or coal could be economically favorable.

## 2.2 Combined carbon dioxide reforming and partial oxidation of methane

In this work, reactant is biogas which consists of methane and carbon dioxide. Oxygen is fed coupled with biogas so the main reactions are carbon dioxide reforming and partial oxidation of methane in order to enhance hydrogen production.

The reforming of methane with carbon dioxide and oxygen was first studied by Vernon et al. (1992). They reported that transition metals supported on inert oxides are active for this reaction. High yields of synthesis gas were obtained without carbon deposition by using a 1%Ir/$Al_2O_3$ catalyst at 1050 K. They were also able to manipulate the $CH_4$:$CO_2$:$O_2$ ratio in order to achieve a thermo-neutral reaction.

Requies et al. (2005) researched on Ni/MgO and Ni/$La_2O_3$ catalysts calcined at temperatures 1073-1273 K. These catalysts were tested in the catalytic partial oxidation of methane at 1073 K. They reported that these catalysts were highly active in the methane partial oxidation reaction. Over $La_2O_3$ substrate, the nickel oxide reacts through solid-state reaction with the near-surface layers of the support particles and forms $LaNiO_3$ as a major Ni-containing phase. This phase becomes reduced to metallic nickel upon activation in $H_2$ flow or under on-stream operation and the finely dispersed Ni metal phase in close contact with the $La_2O_3$ matrix produced appears to be responsible for the catalytic behavior in synthesis gas production. Ni/MgO catalysts are more active and even more stable than the parent Ni/$La_2O_3$ catalysts. The reason for the excellent performance of Ni/MgO catalyst lies in the formation of a cubic (Mg, Ni)O solid solution in which the $Ni^{2+}$ ions are highly stable against reduction even at temperatures as high as 1273 K. Under operation, the small fraction of nickel reduced remains highly dispersed and in close interaction with the basic MgO substrate, this structure being specially suited for synthesis gas production from methane. For both supports, methane conversion increases upon increasing calcination temperature. Long-term activity tests revealed that MgO-supported catalyst, calcined at the highest temperature remains more stable and active than the $La_2O_3$ counterpart.

Choudhary et al. (2000) also studied this reaction over NiO/CaO and NiO/MgO catalyst, conversions above 95% were obtained and the catalyst did not deactivate during 20 h on stream at 1123 K. Ruckenstein et al. (1998) also found that NiO/MgO catalyst has high activity and selectivity, and the formation of a solid solution inhibits the carbon deposition.

The carbon dioxide reforming of methane using various Ni catalysts was investigated by Takano et al. (1994). They reported that the type of support significantly affected the catalytic activity. Ceramic foam and $Al_2O_3$ showed higher activities than $SiO_2$ supports. Alumina-supported catalysts also had stable activities. The addition of MgO to $SiO_2$-supported catalyst increased catalytic activity but decreased stability. Their later work also found that a rapid pressure drop occurred in the plug flow reactor for nickel catalyst by carbonaceous deposition. Catalysts of larger Ni diameter enhanced plugging of the reactor more readily. A macro-porous ceramic support of high porosity decreased this pressure drop.

Several nickel loaded catalysts, $Ni/Al_2O_3$, $Co/Al_2O_3$ and $Fe/Al_2O_3$ in combined carbon dioxide reforming and partial oxidation of methane were reported by Tang et al. (1996). They found that $Ni/Al_2O_3$ is a better catalyst than $Co/Al_2O_3$ and $Fe/Al_2O_3$ as its yields of carbon monoxide and hydrogen are higher than the others. Moreover, nickel catalysts supported on different amounts of SrO modified $SiO_2$ was reported by Jing et al. (2004). They investigated under different temperatures, space velocities and feed gas composition. Results showed that the structure of nickel active phase is strongly dependent on the interaction between nickel and the support, which is related to the support properties, the additives and the preparation methods. They found that SrO modified $Ni/SiO_2$ has a high and stable activity for this reaction, and presented stronger resistance to nickel aggregating, while the unmodified $Ni/SiO_2$ deactivated rapidly from nickel sintering. The enhanced interaction between nickel species and SrO promoted support might be responsible for its high activity and good resistance to agglomeration of the nickel particles.

Keulen et al. (1997) early researched on $Pt/ZrO_2$ catalyst. They reported that it is an active catalyst for the carbon dioxide reforming of methane. However, some deactivation of the catalyst occurred during the first 300 h of a 1000 h test. Then, Aisling et al. (1998) used $Pt/ZrO_2$ catalyst in combined carbon dioxide reforming and partial oxidation of methane. They obtained higher yields of synthesis gas at lower temperature than would be obtained with carbon dioxide reforming of methane alone. Moreover, the loss of activity of the catalyst with time on stream decreased with the amount oxygen added to the feed stream, a small amount of carbon deposition occurred in parts of the catalyst bed which were not exposed to oxygen.

When Pt/$ZrO_2$ catalyst was compared to Pt/$Al_2O_3$ and Pt/10%$ZrO_2$/$Al_2O_3$ catalysts in temperature range of 723-1173 K, it was found that Pt/10%$ZrO_2$/$Al_2O_3$ is the most active and stable catalyst for combined carbon dioxide reforming and partial oxidation of methane. They reported that the carbon deposition during this reaction is influenced by the supports. With small and highly dispersed particles over zirconia-alumina catalyst, the higher stability of the Pt/10%$ZrO_2$/$Al_2O_3$ catalyst is related to its coking resistance, which Pt-$Zr^{n+}$ interacts at metal-support interface.

Additionally, the serious temperature gradient of catalyst bed in combined carbon dioxide reforming and partial oxidation of methane was studied by Tomishige et al. (2002). They reported that Pt/$Al_2O_3$ is much flatter than Ni/$Al_2O_3$ catalyst. Then, Pt-Ni/$Al_2O_3$ catalyst prepared by the sequential impregnation method with small amount of Pt ($0.45\times10^{-5}$ mol/g.cat) exhibited very flat temperature profile in this reaction. Furthermore, the effect of metal loading on Ni/$Al_2O_3$ and Pt/$Al_2O_3$ and Ni catalyst (G-91) on the temperature profile were investigated. Results showed that the temperature at catalyst bed inlet over Pt(10)/$Al_2O_3$ and Pt(1)/$Al_2O_3$ catalysts was much lower than that over Ni(10)/$Al_2O_3$, Ni(30)/$Al_2O_3$, G-91, Pt(0.3)/$Al_2O_3$. This indicates that the combustion and reforming zones overlap in the case of Pt(10)/$Al_2O_3$ and Pt(1)/$Al_2O_3$ catalysts. However, on other catalysts, the zones are separated. In terms of the energy efficiency in the synthesis gas production by methane reforming, the overlap is very effective.

The addition of oxygen to carbon dioxide reforming of methane process was studied by Connor et al. (1998) and also Pan et al. (2002). The results are in good agreement that the addition of oxygen to the feed stream increases methane conversion, especially at temperatures below 1100 K because of the consumption of methane in both carbon dioxide reforming and partial oxidation reactions. On the contrary, when the oxygen contents increases, the carbon dioxide conversion is decreased. However, as the combined carbon dioxide reforming and partial oxidation of methane process is basically a modified carbon dioxide reforming reactions, low temperatures and high oxygen contents are less in this process due to the significant loss in carbon dioxide conversion.

Reforming of methane with carbon dioxide and oxygen involves a coupling of methane oxidation with carbon dioxide reforming in the same reactor. Since, the rate of combustion is much higher than reforming. Therefore, a serious temperature gradient in the catalytic bed is occurred, leading to hot spots. Jing et al. (2004, 2005) studied this reaction over Ni/MgO-$SiO_2$ catalyst and found that a lot of whisker carbon was found on the catalyst in the rear of the fixed bed reactor, but no deposited carbon was observed in fluidized bed reactor after reaction. It leads to enhancement of methane and carbon dioxide conversion. This is suggested that fluidization of catalysts favors inhibiting deposited carbon and thermal uniformity in the reactor. The probable cause is that catalyst particles are circulated between the oxidizing and reducing zones and carbon gasification proceeds in the oxidizing zone.

# CHAPTER III

# THEORY

## 3.1 Reactions for synthesis gas production

The three main industrial chemical reactions for producing hydrogen and synthesis gas from methane are summarized as shown below:

Methane steam reforming reaction

$$CH_4 + H_2O \longrightarrow CO + 3H_2 \qquad \Delta H^{\circ}_{298} = 206 \text{ kJ/mol} \qquad (3.1)$$

Methane partial oxidation with oxygen

$$CH_4 + 1/2O_2 \longrightarrow CO + 2H_2 \qquad \Delta H^{\circ}_{298} = -36 \text{ kJ/mol} \qquad (3.2)$$

Methane dry reforming with carbon dioxide

$$CH_4 + CO_2 \longrightarrow 2CO + 2H_2 \qquad \Delta H^{\circ}_{298} = 261 \text{ kJ/mol} \qquad (3.3)$$

From downstream synthesis, different $H_2$/CO ratio in the synthesis gas contributes to different desired products, as shown in Table 3.1

**Table 3.1** Required $H_2$/CO ratio of different desired products (Japan Petroleum Energy Center, 1999)

| **Desired product** | **Required $H_2$/CO ratio** |
|---|---|
| Synthetic Oil | 1/2 - 2/1 |
| Methanol | 2/1 |
| Acetic Acid | 1/1 |
| Glycol | 3/2 |
| Acetyloxide | 1/1 |
| Propionic Acid | 4/3 |
| Methacrylic Acid | 5/4 |
| Ethanol | 2/1 |
| Acetaldehyde | 3/2 |
| Acetic Ethene | 5/4 |
| Acetic Ether | 3/2 |
| Ethene | 2/1 |

### 3.1.1 Steam reforming

Methane steam reforming is the most common way of producing hydrogen including carbon monoxide. The hydrogen product is used in the industrial synthesis of ammonia. It is also the cheapest method. At high temperatures (973 – 1373 K) and in the presence of a metal-based catalyst (nickel), steam reacts with methane to form carbon monoxide and hydrogen yield. The hydrogen to carbon monoxide ratio is high and this reaction is extremely endothermic. Steam reforming offers an efficient, economical, generally used process for hydrogen production and environmental benefits. The efficiency of this process is approximately 65% to 75%.

$$CH_4 + H_2O \rightarrow CO + 3H_2 \qquad \Delta H^\circ_{298} = 206 \text{ kJ/mol}$$

Additionally, the yield of hydrogen can be improved by water gas shift reaction. The water gas shift reaction was discovered by Italian physicist Felice Fontana in 1780. This reaction is an essential industrial reaction which carbon monoxide reacts with water to form carbon dioxide and hydrogen. It is often used in combination with methane steam reforming or other hydrocarbons which is important for the high purity hydrogen production for use in ammonia synthesis. The reaction is slightly exothermic. However, thermodynamic equilibrium favors high conversion of CO and steam to hydrogen and carbon dioxide at low temperatures. Therefore, the water-gas shift reaction is normally performed at low temperature in the presence of catalysts that enhance the reaction rate.

$$CO + H_2O \rightarrow CO_2 + H_2 \qquad \Delta H^\circ_{298} = -40 \text{ kJ/mol}$$

Moreover, the water gas shift reaction is sensitive to temperature and tends to shift towards reactants which are carbon monoxide and water when temperature increases due to Le Chatelier's principle. In fuel-rich hydrocarbon combustion processes, the water gas shift reaction at equilibrium state is often employed as a means to provide approximates for molar concentrations of burnt gas components. This reaction is often used in two stages. First stage is a high temperature shift (HTS) at 623 K and Second stage is a low temperature shift (LTS) at 463-483 K.

### 3.1.2 Catalytic partial oxidation

This reaction is slightly exothermic and energy consumption is lower than in of methane steam reforming which is endothermic reaction.

$$CH_4 + 1/2O_2 \rightarrow CO + 2H_2 \qquad \Delta H^\circ_{298} = -36 \text{ kJ/mol}$$

Because the reaction speed is rapid, the reactor is particularly small. In comparison to the non-catalytic partial oxidation reaction, there is no generation of soot or other unnecessary by-products. Because the addition of little water results in synthesis gas with $H_2$/CO ratio of 2, the reaction is ideal for producing synthesis gas for Fischer-Tropsch synthesis or methanol production. In addition, equipment costs are reduced by about 30% from conventional reactions.

A significant disadvantage in catalytic partial oxidation and methane steam reforming is the possible occurrence of carbon deposition, via the Boudouard reaction (Eq. 3.4), decomposition of methane (Eq. 3.5), and the CO reduction reaction (Eq. 3.6):

$$2CO \leftrightarrow C + CO_2 \qquad \Delta H^\circ_{298} = -171 \text{ kJ / mol} \qquad (3.4)$$

$$CH_4 \leftrightarrow C + 2H_2 \qquad \Delta H^\circ_{298} = 89.9 \text{ kJ / mol} \qquad (3.5)$$

$$CO + H_2 \leftrightarrow C + H_2O \qquad \Delta H^\circ_{298} = -136 \text{ kJ / mol} \qquad (3.6)$$

The Boudouard and CO reduction reactions which are highly exothermic reactions are clearly preferred at low temperature and high pressure. In contrast, methane decomposition is favored at high temperature and low pressure. Carbon deposition should always be minimized, because it contributes to catalyst deactivation and plugging in the reactor.

### 3.1.3 Reaction route of catalytic partial oxidation

From Figure 3.1, the catalytic partial oxidation reaction route consists of direct route and two-stage route. In the direct route, carbon monoxide and hydrogen are produced directly from methane. In the two-stage route, complete combustion of methane takes place at first, then synthesis gas is produced by following methane steam reforming, dry reforming with carbon dioxide, or by the advance of water gas shift reaction.

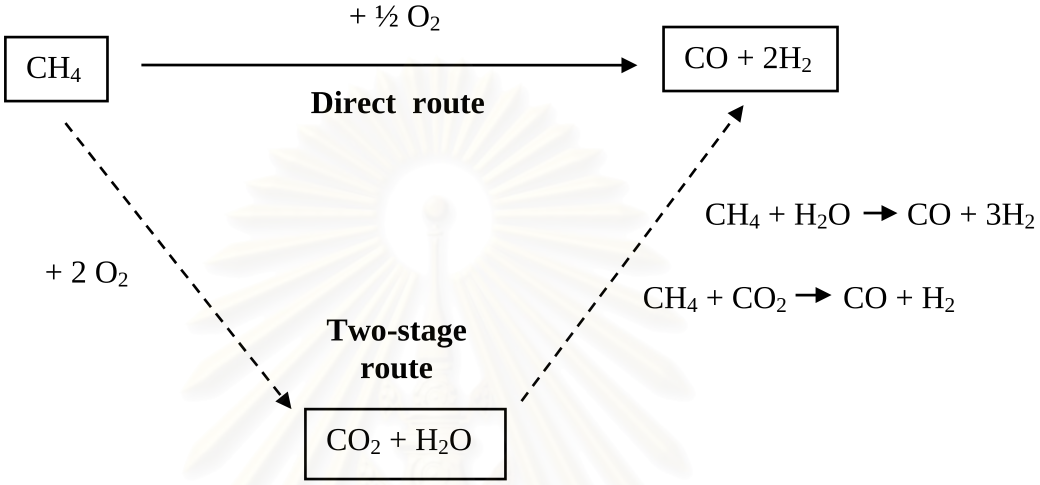

**Figure 3.1** Reaction route diagram (Japan Petroleum Energy Center, 1999)

### 3.1.4 Economy of catalytic partial oxidation

An evaluation of the economy of synthesis gas production which consists of five reactions is showed in Table 3.2. The estimation was based on a comparison of economy in the production of 2,500 tons/day of methanol. Comparisons were made with other devices, taking the steam reforming reaction as 100. Superiority in economy was concluded to be in the following sequence: catalytic partial oxidation (CPOX), compound reforming reaction (CR), autothermal reforming reaction (ATR), (non catalytic) partial oxidation (POX) and steam reforming reaction (SMR). It was presented that costs from catalytic partial oxidation were 30% lower than from the steam reforming reaction. The same trend was shown in the decrease of carbon dioxide gas emissions, the main factor in the phenomenon of global warming. It was exhibited that emissions from the catalytic partial oxidation were 35% lower than from the steam reforming reaction (Japan Petroleum Energy Center, 1999).

**Table 3.2** Comparison of economy by reforming reaction (Japan Petroleum Energy Center, 1999)

| | *SMR* | *POX* | *ATR* | *CR* | *CPOX* |
|---|---|---|---|---|---|
| Natural gas Consumption volume (GJ/t-MeOH) | 32 | 31.6 | 30.6 | 30 | (29-30) |
| Oxygen consumption Volume ($m^3$/t-MeOH) | | 530 | 460 | 280 | 270-300 |
| $CO_2$ emissions Volume ($10^3$ t/y) | 380 | 375 | 355 | 290 | 250-270 |
| Relative costs | 100 | 95 | 85-95 | 80-85 | 70-80 |

### 3.1.5 Thermodynamics of carbon dioxide reforming of methane

The carbon dioxide reforming of methane (or methane dry reforming) was first studied by Fischer and Tropsch (1928) over a number of base metal catalysts. Calculations indicate that the reaction is thermodynamically favored above 913 K. It is more endothermic than methane steam reforming reaction (Promaros, 2005).

Methane dry reforming with carbon dioxide (Eq. 3.3) which is a highly endothermic reaction has similar thermodynamic and equilibrium characteristics to methane steam reforming reaction (Eq. 3.1). However, synthesis gas production has a lower $H_2$/CO ratio. Methane steam reforming is obviously favored at high temperature because it is endothermic. In addition, methane steam reforming is favored at low pressure because it is accompanied by a volume expansion.

Methane dry reforming with carbon dioxide is prone to be conducted under conditions where carbon formation via decomposition of methane (Eq. 3.7) and/or Boudouard reaction (Eq. 3.8) is thermodynamically practical.

$$CH_4 \rightarrow C + 2H_2 \qquad \Delta H^\circ_{298} = 75 \text{ kJ/mol} \qquad (3.7)$$

$$2CO \rightarrow C + CO_2 \qquad \Delta H^\circ_{298} = -171 \text{ kJ/mol} \qquad (3.8)$$

Other reactions which could have an important effect on the overall product are:

$$CO_2 + H_2 \rightarrow CO + H_2O \qquad \Delta H^\circ_{298} = 40 \text{ kJ/mol} \qquad (3.9)$$

$$C + H_2O \rightarrow CO + H_2 \qquad \Delta H^\circ_{298} = 131 \text{ kJ/mol} \qquad (3.10)$$

The formation of solid carbon should always be minimized because it leads to catalyst deactivation and plugging problem in the reactor. Theoretically, the carbon formed in reaction (Eq. 3.7) should be rapidly consumed by the reverse of reaction (Eq. 3.8), and by the steam to carbon gasification reaction (Eq. 3.10). Practically, steam is almost always formed via the reverse water gas shift reaction (RWGS) (Eq. 3.9). If the decomposition of methane reaction is faster than the carbon removal rate, carbon deposition is serious problem in the overall reaction. However, it should be noted that the formation of water is not desired in this reaction system as it reduces the selectivity of hydrogen.

### 3.1.6 Reaction mechanism of carbon dioxide reforming of methane

The reaction mechanism of methane dry reforming with carbon dioxide has been explored by many researchers. Solymosi et al. (1991, 1993) proposed the possible mechanism of methane dry reforming with carbon dioxide over supported metal catalyst. Activation of methane would be produced via dissociation of methane with activation carbon, which is formed at the end of reaction as follows:

$$CH_4 \rightarrow CH_3^* + H^*, \qquad (3.11)$$

$$CH_3^* \rightarrow CH_2^* + H^*, \qquad (3.12)$$

$$CH_2^* \rightarrow CH^* + H^*, \qquad (3.13)$$

$$CH^* \rightarrow C^* + H^*. \qquad (3.14)$$

Normally, many forms of carbon depositions are different in reactivity: adsorbed atomic carbon which is a highly reactive form, amorphous carbon, vermicular carbon, bulk nickel carbide, and crystalline graphitic carbon. The reactivity of deposited carbon depends on the type of catalytic surface, the temperature of its formation and the duration of thermal treatment. Carbon is formed from carbon monoxide as the precursor as shown by reaction (Eq. 3.16).

$$CO_2 \rightarrow CO^* + O^* \qquad (3.15)$$

$$CO^* \rightarrow C^* + O^* \qquad (3.16)$$

Unless both methane and carbon dioxide can dissociate separately, their deposited products terminate the respective dissociation by covering the metal surfaces. The self-decomposition of both methane and carbon dioxide could be facilitated via reactions (Eq. 3.17) to (Eq. 3.19). The dissociation of methane is enhanced by adsorbed oxygen, while the dissociation of carbon dioxide is also promoted by adsorbed hydrogen and other methane residues. Therefore, the reactions of these surface species also would like to be investigated as the following reactions:

$$CO_2 + H^* \rightarrow CO^* + OH^* \qquad (3.17)$$

$$CH_4 + O^* \rightarrow CH_3^* + OH^* \qquad (3.18)$$

$$CH_x + O^* \rightarrow CH_3^* + OH^* \qquad (3.19)$$

$$2OH \rightarrow H_2O^* + O^* \qquad (3.20)$$

### 3.1.7 Thermodynamics of combined carbon dioxide reforming and partial oxidation of methane

The combination of methane dry reforming with carbon dioxide and partial oxidation is a complex multi-reaction network system, which consists of various major reactions as summarized in Eq. 3.21-3.25:

$$CH_4 + \tfrac{1}{2} O_2 \rightarrow CO + 2H_2 \qquad \Delta H^\circ_{298} = -36\ \text{kJ/mol} \qquad (3.21)$$

$$CH_4 + 2O_2 \rightarrow CO_2 + 2H_2O \qquad \Delta H^\circ_{298} = -802\ \text{kJ/mol} \qquad (3.22)$$

$$CH_4 + CO_2 \rightarrow 2CO + 2H_2 \qquad \Delta H^\circ_{298} = 261\ \text{kJ/mol} \qquad (3.23)$$

$$CH_4 + H_2O \rightarrow CO + 3H_2 \qquad \Delta H^\circ_{298} = 206\ \text{kJ/mol} \qquad (3.24)$$

$$CO_2 + H_2 \rightarrow CO + H_2O \qquad \Delta H^\circ_{298} = 40\ \text{kJ/mol} \qquad (3.25)$$

This process can produce synthesis gas with $H_2$/CO ratios about 1, which is suitable for production of oxygenated compounds, heavy hydrocarbons by Fischer-Tropsch synthesis and carbon monoxide for synthesis of polycarbonates. The addition of oxygen feed to the methane dry reforming with carbon dioxide can decline the formation of carbon on the catalytic surface and increase methane conversion, although this can also cause the reduction of process selectivity. Moreover, as the methane oxidation is highly exothermic, the temperature control of reactor may be very difficult at certain conditions which contribute to the formation of hot spots. The addition of carbon dioxide feed to the partial oxidation reaction can improve the temperature control of reactor and decrease the formation of hot spots.

### 3.1.8 Catalyst for combined carbon dioxide reforming and partial oxidation of methane

The noble metals such as Ni, Ru, Rh, Pd, Ir, and Pt are used as the active metal in catalysts. Determining the overall performance criteria, Rh is a better material which is high activity, high hydrogen selectivity and carbon-free operation. However, Rh is too expensive to utilize practically. Due to cheap metal, Ni is the most widely used metal from this group. The main drawback of a conventional Ni-based catalyst is its poor stability, mainly caused by carbon formation and less active which is showed in Table 3.3.

**Table 3.3** Relative activities for steam reforming of methane. T=550°C, S/C=4, P=1 bar (Rostrup-Nielsen and Hansen, 1993)

| Catalyst metal content (wt%) | Relative rate |
|---|---|
| Ni (16) | 1.0 |
| Ru (1.4) | 2.1 |
| Rh (1.1) | 1.9 |
| Pd (1.2) | 0.4 |
| Ir (0.9) | 1.1 |
| Pt (0.9) | 0.5 |

The activity of a catalyst is related to the metal surface. This implies that the catalytic activity benefits from a high dispersion of the metal particles. The structure of the available surface area also strongly influences the catalyst activity. For example, the close-packed (111) surface of nickel is less active than the more open (110) surface. In fact, metal atoms in surface steps and near defects are more reactive than metal atoms in the higher coordinated surface terrace sites. For instance, it is known that Ni particles are composed of a number of single crystals; i.e., the metal particles are polycrystalline. However, they are not completely space filling. Therefore, some lattice distortion is required and these dislocations are expected to play a role in the catalytic reaction.

The role of the catalyst support is to provide a support for the catalytically active metal, in order to obtain a stable and high active surface area. The common supports for methane reforming are α- and γ-$Al_2O_3$, MgO, $MgAl_2O_4$, $SiO_2$, $ZrO_2$, and $TiO_2$. These supports have good porosity, which results in a long contact-time between reactants and catalyst. Sustaining a high active surface area is also important. The support can affect the migration and coalescence of metal particles in various methods. Pore structure, morphology, and phase transitions of the support determine the final particle size of the metal. However, with using the same kind of catalyst support and active component, the difference in catalyst preparation methods would result in different surface morphology of the obtained catalysts. Changing catalyst preparation method can cause different sintering resistant, e.g., from calcinations. It should be noted that for the evaluation of catalyst stability it is essential to consider the effect of sintering under reaction conditions. The support may also actively participate in the catalytic reaction itself. For instance, supports with a basic nature, such as MgO, are known to enhance the activation of steam (i.e., dissociation into reactive OH and H species). Also, stabilization of different $CH_x$-intermediates contributes to the overall reaction mechanism.

### 3.2 Sorption Enhanced Reaction Process

The in-situ removal of $CO_2$ can be advantageous when used in equilibrium-limited reactions that produce $CO_2$ as a by-product. The processes where in situ separation of one or more products is performed in the reaction chamber are called sorption enhanced reaction processes (SERP) (Oliveira et al., 2008).

SERP combines reaction and separation in a single unit operation (such as adsorptive reactor, chromatographic reactor, membrane reactor, etc.). Thus sorption enhanced reaction process can result in process simplification, improved energy efficiency, and enhanced reactant conversion and product yield (Xiu et al., 2002).

The materials which are of interest for SERP which was researched by Reijers et al. (2006) can be divided into the following five groups:

(1) metal oxides
(2) hydrotalcites
(3) double salts
(4) lithium metal oxides
(5) supported sorbents

At first, metal oxides which like CaO and MgO react chemically with $CO_2$. Then, hydrotalcites also called layered double hydroxides or Feitknecht compounds, belong to the family of anionic clays. Then, potassium double salts were identified as the active phase in the decomposition products of $K_2CO_3$-impregnated hydrotalcite using high-temperature X-ray diffraction. The preparation of synthesizing double salts as a side product by decomposition of hydrotalcite resulted in sorbents having higher adsorption capacity and improved kinetics compared with promoted hydrotalcites. After that, lithium metal oxides were discovered by Toshiba while they added $ZrO_2$ to the molten electrolyte in their molten carbonate research. The product from their research, $Li_2ZrO_3$, was found to be a good $CO_2$ sorbent, as were other lithium metal oxides. Finally, supported sorbents are the combinations of a sorbent of groups (1)-(4) and a suitable support material. For example, CaO was supported by Cabot Superior Micropowder. The properties of the above five groups of sorbents are summarized in Table 3.4. Those sorbent materials which are used for $CO_2$ removal at other conditions are excluded. Materials such as zeolites, amines, carbonates, and active carbon are used at relatively low temperatures (mainly lower than 373 K). Thus, they were not taken into consideration. The stability of double salts has not been investigated very well because a good recipe for a binder in order to produce pellets from the precipitates has not been found yet. Trying to select a sorbent from the remaining four on the basis of this table proves hard because the overall performance of the various sorbent groups is quite similar. Therefore, system aspects need to be taken into account as well. Note that, of these five groups, the materials of the first and fourth groups are preferably regenerated by temperature swing because they react with $CO_2$ in a significantly exothermic reaction ($\Delta H$ = 170 kJ/ mol for CaO at 1073K, $\Delta H$ = 170 kJ/mol for $Li_4SiO_4$ at 973 K). Those of the second and third groups can be regenerated by pressure swing because the heat of adsorption is relatively low (17 kJ/mol). Those of the last group may be regenerated using either temperature or pressure swing which depend on the sorbent material. Obviously, the chosen regeneration method (temperature swing or pressure swing) has important consequences for the system configuration and efficiency.

**Table 3.4** Characteristics of $CO_2$ sorbent materials (Reijers et al., 2006)

| group | representative member | adsorption capacity | stability | kinetics |
|---|---|---|---|---|
| Metal oxide | CaO | good | poor | good |
| hydrotalcites | $Mg_6Al_2(OH)_{16}[CO_3].4H_2O/K_2CO_3$ | poor | good | poor |
| double salts | $(K_2CO_3)(2KHCO_3)(MgCO_3)(MgO).xH_2O$ | fair | unknown | fair |
| Li metal oxides | $Li_4SiO_4$ | fair | fair | good |
| supported sorbents | CaO on Cabot Superior Micropowder | fair | good | good |

### 3.2.1 Calcium oxide sorbent

Calcium oxide (CaO) commonly known as burnt lime, lime or quicklime, is a widely used chemical compound. It is a white, caustic and alkaline crystalline solid. Structure and properties of calcium oxide are shown in Fig 3.2 and Table 3.5, respectively. As a commercial product, lime often also contains magnesium oxide, silicon oxide and smaller amounts of aluminium oxide and iron oxide.

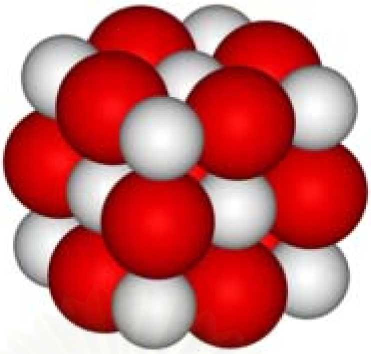

**Figure 3.2** Structure of calcium oxide

**Table 3.5** Properties of calcium oxide

| Properties | |
|---|---|
| Molecular formula | CaO |
| Molar mass | 56.077 g/mol |
| Appearance | Fine white solid |
| Density | 3350 kg/m$^3$, solid |
| Melting point | 2572 $^o$C (2845 K) |
| Boiling point | 2850 $^o$C (3123 K) |
| Solubility in water | Reacts |

Calcium oxide is usually produced by the thermal decomposition of materials such as limestone which contain calcium carbonate ($CaCO_3$; mineral name: calcite) in a lime kiln. This is accomplished by heating the material to above 1098 K, a process called calcination or lime-burning (Eq. 3.31). A molecule of carbon dioxide ($CO_2$) is released from CaO sorbent. This process is greatly endothermic.

$$CaCO_3 \longrightarrow CaO + CO_2 \qquad \Delta H°_{298} = 178 \text{ kJ/mol} \qquad (3.31)$$

Calcination is reversible. When CaO product has cooled, it immediately begins to absorb carbon dioxide from the air, until, after enough time, and it is completely converted back to calcium carbonate, a process called carbonation (Eq. 3.32). Carbonation is highly exothermic.

$$CaO + CO_2 \longrightarrow CaCO_3 \qquad \Delta H°_{298} = -178 \text{ kJ/mol} \qquad (3.32)$$

# CHAPTER IV

# EXPERIMENTAL

## 4.1 Chemicals and Materials

### 4.1.1 Catalyst

The catalyst used in the present work is Ni/$SiO_2$.MgO (commercial grade) obtained from Japan. This catalyst was applied in sorption-enhanced operation of combined carbon dioxide reforming and partial oxidation of biogas. The shape of catalyst is solid cylindrical extrudate with a diameter of three millimeters and three millimeters in length. More details of the catalyst characteristics are presented in Table 4.1.

**Table 4.1** The specific properties of catalyst used in the experiment

| **Catalyst** | **Ni/$SiO_2$.MgO** |
|---|---|
| Ni content | 55 %w/w |
| Support/co-catalyst | $SiO_2$, MgO |
| Surface area [$m^2$/kg] | $1.21 \times 10^5$ |
| Ni Surface area [$m^2$/kg] | $8.37 \times 10^3$ |
| Ni diameter [nm] | 44 |

### 4.1.2 Sorbent

CaO (commercial grade) used in the present work is supplied by Riedel-de Haën. This sorbent was packed with catalyst in different modes in order to combine reaction and sorption in a single unit operation. This sorbent is fine white powder with characteristics as listed below.

**Table 4.2** Specific properties of CaO sorbent

| **Analytical specification** | **Content** |
|---|---|
| Assay | 96 – 100.5% |
| Insoluble in HCl | Max. 0.5% |
| Loss on ignition | Max. 3.5% |
| As max. 0.0003% Pb | Max. 0.0005% |
| Heavy metals (as Pb) | Max. 0.003% |
| Fluoride (F) | Max. 0.015% |
| Mg and alkali salts ($SO_4$) | Max. 2.5% |

### 4.1.3 Dilution material

A dilution material was used for uniformly mixing with catalyst before packing in the reactor in order to reduce the bed pressure drop due to carbon formation from the reaction and to reduce temperature gradients along the catalyst bed. Silicon dioxide ($SiO_2$) supplied by Fluka was chosen as a dilution material for this research. The average size of silicon dioxide was 40-100 mesh.

### 4.1.4 Reactant gases

The details of gases used to study the sorption-enhanced operation of combined carbon dioxide reforming and partial oxidation of biogas are illustrated in Table 4.3.

**Table 4.3** Reaction gases used for the experiment

| **Gas** | **Grade** | **Supplier** |
|---|---|---|
| Methane | Grade 4 | TIG |
| Carbon dioxide | Ultra high pure | TIG |
| Oxygen | High pure | TIG |
| Hydrogen | Ultra high pure | TIG |
| Argon | Ultra high pure | TIG |

## 4.2 Apparatus

### 4.2.1 Reactor

The reaction was performed in a conventional quartz tube with an inside diameter of 11 millimeters at atmospheric pressure. The quartz tube reactor was placed in the vertical direction with downward gas flow. There were two sampling points located before and after the catalyst bed. Catalyst was placed over quartz wool, which was packed for supporting the catalyst bed. The diagram of a lab-scale gas phase for the sorption-enhanced operation of combined carbon dioxide reforming and partial oxidation of biogas is exhibited schematically in Figure 4.1.

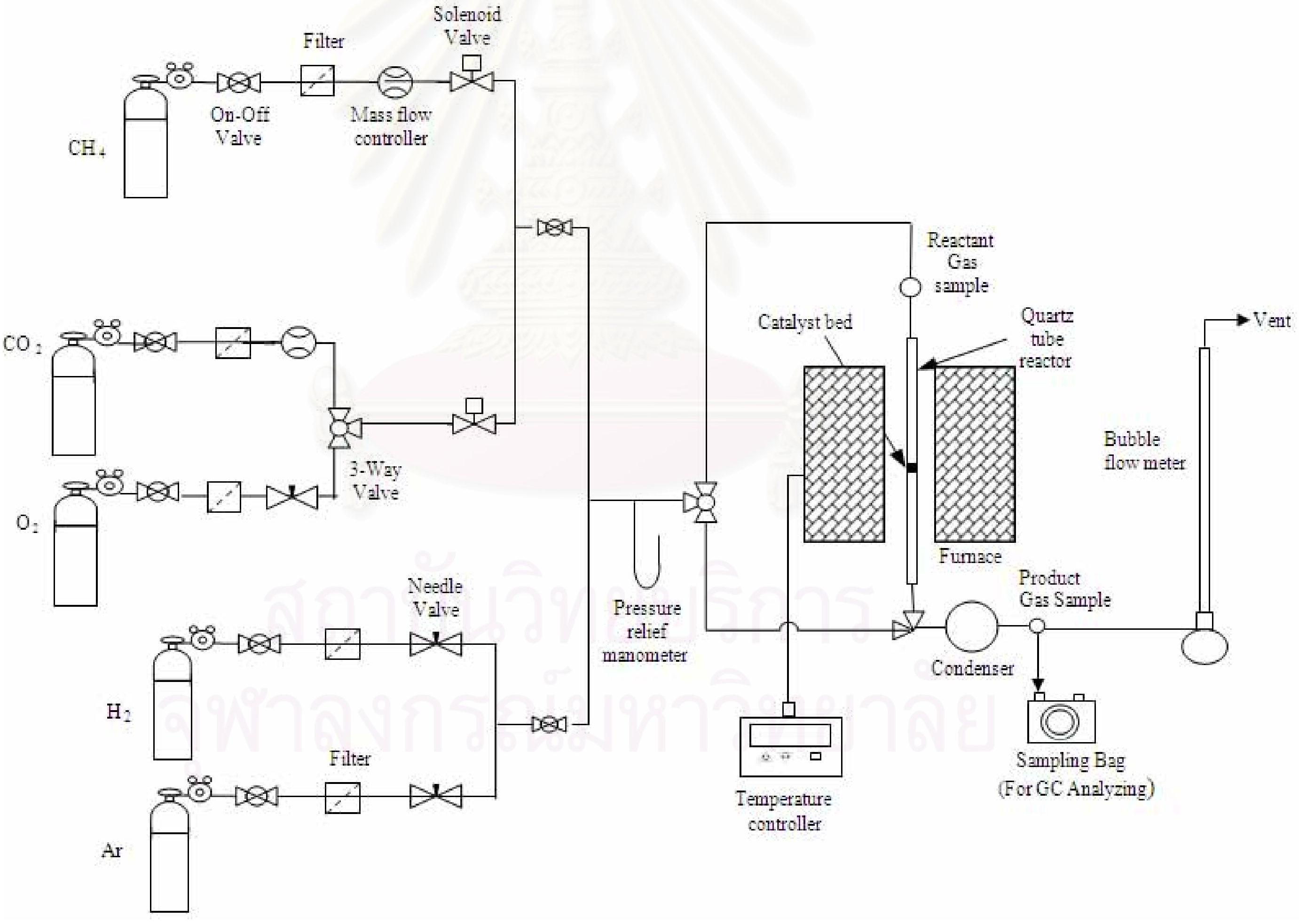

**Figure 4.1** Schematic diagram of a lab-scale gas phase for the sorption-enhanced operation of combined carbon dioxide reforming and partial oxidation of biogas.

### 4.2.2 Automatic Temperature Controller

This unit consists of a magnetic solid state relay switch connected to a variable voltage transformer and a temperature controller connected to a thermocouple. Reactor temperature was measured by thermocouple which was placed in the furnace at the position of the catalyst bed. The temperature control set point is adjustable within the range of room temperature to 1273 K at the maximum voltage output of 220 V.

### 4.2.3 Electrical Furnace

The furnace with 1.5 kW heating coil was connected with the automatic temperature controller to supply heat to the reactor. The reactor could be operated from room temperature up to 1273 K at the maximum voltage of 220 V.

### 4.2.4 Gas Controlling System

Each reactant gas was equipped with a pressure gas regulator (0-120 psig) and an on-off valve. The flow rate was controlled by mass flow controller (GFC17S) operated under the flow range between 0-50 mL/min.

### 4.2.5 Gas Chromatography

A gas chromatography Shimadzu modal 8A (GC-8A) equipped with a thermal conductivity detector (TCD) was used to analyze gas composition. Methane and oxygen in feed streams, carbon monoxide and hydrogen in the product streams were analyzed using Molecular sieve 5A column. Carbon dioxide in the product stream was analyzed by using Poropak-Q column. The operating conditions for the gas chromatography are given in Table 4.4.

**Table 4.4** Operating conditions of gas chromatography for sorption-enhanced operation of combined carbon dioxide reforming and partial oxidation of biogas

| Gas Chromatography | SHIMADZU GC 8A | |
|---|---|---|
| Detector | TCD | |
| Packed column | Molecular sieve 5A | Porapak-Q |
| - Column material | SUS | SUS |
| - Length (m) | 2 | - |
| - Outer diameter (mm) | 4 | - |
| - Inner diameter (mm) | 3 | - |
| - Mesh range | 60/80 | - |
| - Maximum temperature (K) | 623 | - |
| Carrier gas | Ultra high purity Ar | Ultra high purity Ar |
| Carrier gas flow rate (mL/min) | 40 | 40 |
| Injector temperature (K) | 373 | 373 |
| Detector temperature (K) | 373 | 373 |
| Column temperature | | |
| - initial (K) | 343 | 343 |
| - final (K) | 343 | 343 |
| Current (mA) | 70 | 70 |
| Analyzed gas | $CH_4$,$O_2$, $H_2$, CO | $CO_2$ |

## 4.3 Experimental procedures

The objective of this experimental study is to investigate the potential benefits of utilizing CaO as a $CO_2$ sorbent in the combined carbon dioxide reforming and partial oxidation of biogas for hydrogen production. Three different bed arrangements in the sorption-enhanced operation; i) Ni/$SiO_2$.MgO before CaO, ii) CaO before

Ni/SiO$_2$.MgO and iii) mixture of CaO and Ni/SiO$_2$.MgO, is compared with that of the conventional system without CaO sorbent which are depicted in Figure 4.2.

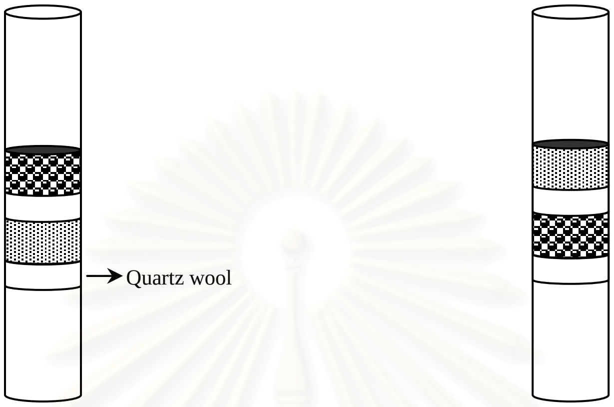

i) Ni/SiO$_2$.MgO before CaO

ii) CaO before Ni/SiO$_2$.MgO

iii) mixture of CaO and Ni/SiO$_2$.MgO

iv) without CaO sorbent

**Figure 4.2** Three different bed arrangements in the sorption-enhanced operation compared with that of the conventional system without CaO sorbent

For the conventional system without CaO, the catalyst was prepared by mixing 0.1314 g of Ni/SiO$_2$.MgO with 0.438 g of SiO$_2$ (dilution material). The mixture of catalyst was packed in the middle of the reactor and then placed in the electrical furnace. Before starting the reaction, the reduction of catalyst under hydrogen flow was conducted.

For three different bed arrangements in the sorption-enhanced system, the catalyst was prepared by mixing 0.1314 g of Ni/$SiO_2$.MgO with 0.438 g of $SiO_2$ (dilution material). The CaO sorbent (0.657 g) was packed with catalyst. Before starting the reaction, the reduction of catalyst under hydrogen flow was conducted.

Reduction step:

The reactor was heated up to 923 K in argon flow of 30 mL/min. When the temperature reached to 923 K, the argon gas was switched off and the catalyst was reduced in hydrogen flow of 30 mL/min for 1 hour. After that, the system was purged in argon flow again for 10 minutes to remove hydrogen gas from the system.

Reaction step:

For steady state operation, the reaction was started by introducing $CH_4$, $CO_2$ and $O_2$ simultaneously to the reactor at reaction temperature 1023 K under total pressure of 1 atm. The molar flow rates of reactant gases are showed in Table 4.5. The gas sampling from product stream was taken every 10 minutes to analyze its composition by the TCD gas chromatography.

**Table 4.5** The molar flow rates of reactant gases used for steady state operation

| Reactants | Flow rate (mL/min) |
|---|---|
| **$CH_4$** | 12.5 |
| **$CO_2$** | 12.5 |
| **$O_2$** | 6.25 |

# CHAPTER V

# RESULTS AND DISCUSSION

This work studies the sorption-enhanced combination of carbon dioxide reforming and partial oxidation of biogas over a mixture of industrial steam reforming $Ni/SiO_2.MgO$ catalyst and CaO adsorbent. The results and discussions in this chapter are divided into three main parts. In the first part, a set of experiments was carried out to investigate the effect of adsorbent and catalyst bed arrangement on the combined carbon dioxide reforming and partial oxidation of biogas. The second part based on simulations, the effects of temperature, oxygen, water and CaO sorbent on the combined carbon dioxide reforming and partial oxidation of biogas carried out in a fluidized bed reactor were investigated. In the last part, the operating conditions which offer thermal-neutral operation were presented. The results of both the second and last parts were investigated by using Aspen Plus Simulator.

## 5.1 The effect of different adsorbent and catalyst bed arrangement.

This part concentrated on the effect of different adsorbent and catalyst bed arrangement. The methane, carbon dioxide and oxygen flow rates were set constant at 12.5, 12.5 and 6.25 mL/min, respectively. The reaction was operated at 1023 K and atmospheric pressure under continuous feeds of the reactants. The catalytic performance of the reactor in term of hydrogen yield was determined.

The results of hydrogen yield from 4 different runs were shown in Figure 5.1. The reaction temperature was kept at 1023 K under atmospheric pressure. For the case without CaO (conventional operation), it is observed that the hydrogen yield initially increases and levels off at a hydrogen yield of about 57%. The case with $Ni/SiO_2.MgO$ before CaO shows similar behavior as the case without CaO, indicating that the presence of CaO after the catalyst bed does not help improve the reactions in the system. However, it is observed that the hydrogen concentration in the exit gas becomes higher than the conventional case (not shown) because $CO_2$ in the reaction product is adsorbed by CaO. The improved hydrogen yield is observed for the cases with CaO before Ni/$SiO_2$.MgO and mixture of CaO and Ni/$SiO_2$.MgO. When packing CaO before the catalyst, some $CO_2$ is removed from the feed gas before the main reactions taking place in the subsequent catalyst bed. The improved hydrogen yield is observed for 20 min of reaction time. When CaO is mixed with the catalyst in the bed, the improvement of hydrogen yield becomes more significant and the superior yield is observed until 80 min of reaction time. It should be noted that for all reaction runs, after extended reaction operation, the hydrogen yields approach the same value of about 57%. This is because the adsorption of $CO_2$ by CaO becomes insignificant as most CaO is converted to $CaCO_3$. From the preliminary results it is obvious that the use of CaO in the combined carbon dioxide reforming and partial oxidation of biogas particularly for the mode of mixture of CaO and Ni/$SiO_2$.MgO can improve the hydrogen yield over the conventional system. Therefore, the reaction system with the mode of mixture of CaO and Ni/$SiO_2$.MgO is considered in the following studies. In order to enable the operation under steady state condition, a fluidized bed reactor with continuous feeds of a gas mixture and CaO is proposed. When this reactor is equipped with a regenerator for regenerating $CaCO_3$ into CaO, the system can be operated under continuous and steady-state condition presented in Figure 5.2. In addition, the removed $CO_2$ can be further sequestrated, if necessary, in order to reduce the amount of $CO_2$ released to the environment. The following study will focus only on the fluidized bed reactor without the presence of CaO regenerator.

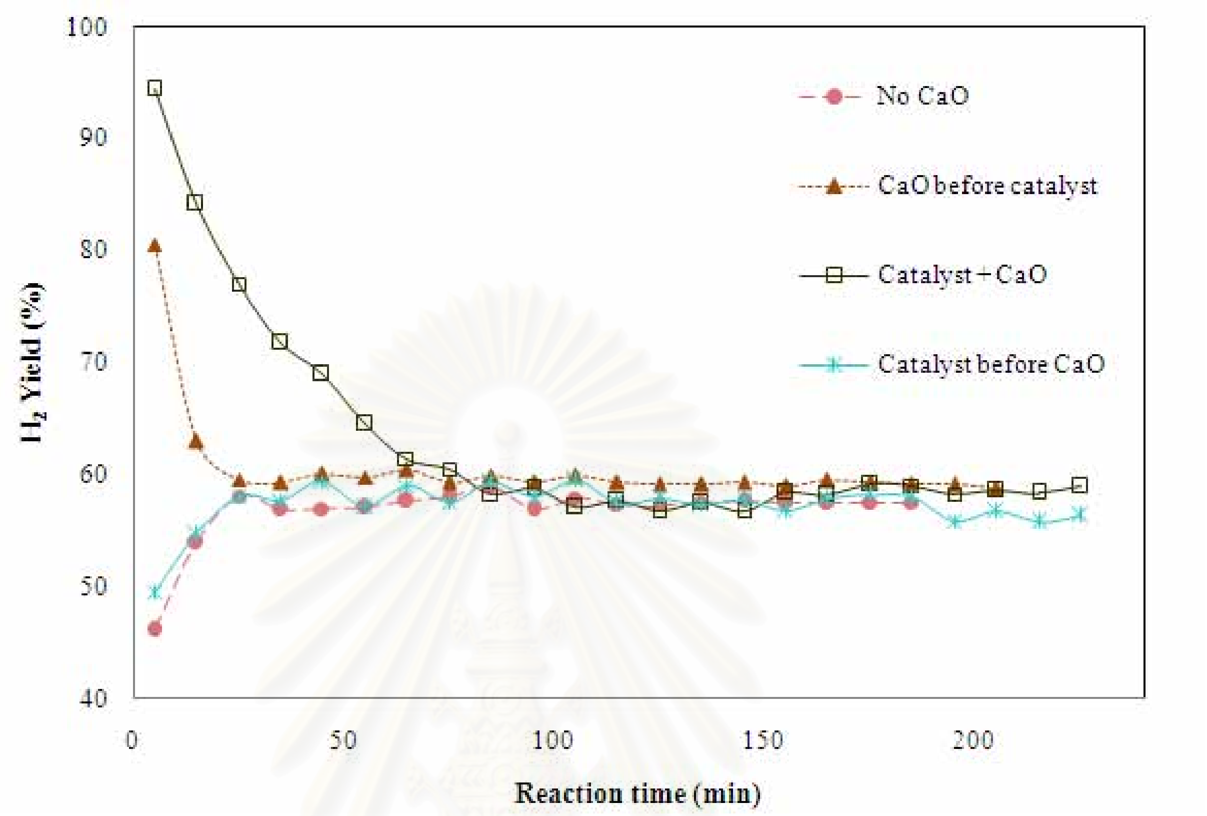

**Figure 5.1** Hydrogen yield in combined carbon dioxide reforming and partial oxidation of biogas under steady state operation at 1023 K with different adsorbent and catalyst bed arrangement.

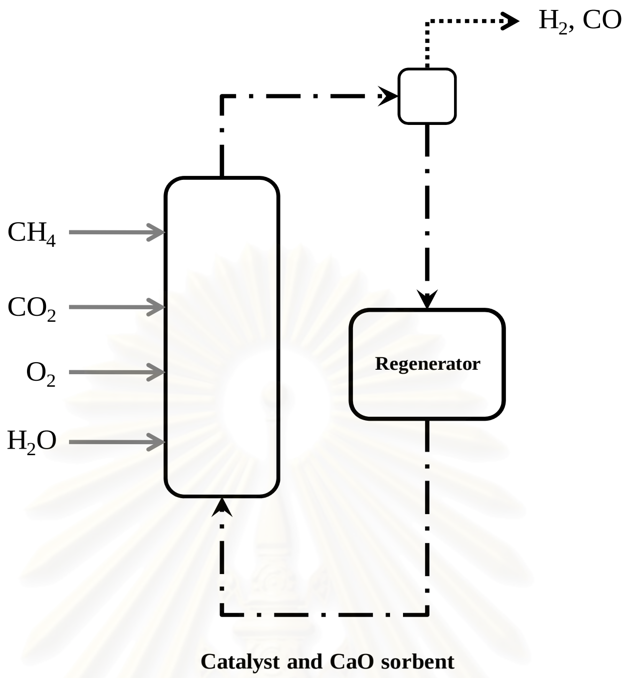

**Figure 5.2** The system can be operated under continuous and steady-state condition.

## 5.2 The effects of the addition of oxygen, water, calcium oxide (CaO) sorbent and temperature on reaction.

This part studied the effects of the addition of oxygen, water, CaO sorbent and temperature on the combined carbon dioxide reforming and partial oxidation of biogas in the system proposed in the previous section. The study was carried out by simulations assuming equilibrium reactions. The methane and carbon dioxide flow rates were set constant at 1 mol/s while the $O_2/CH_4$, $H_2O/CH_4$, $CaO/CH_4$ ratios and the reaction temperature were varied.

Firstly, the effects of the oxygen addition on hydrogen yield, hydrogen concentration, hydrogen: carbon monoxide ratio and the overall enthalpy in the combined carbon dioxide reforming and partial oxidation of biogas were presented in Figures 5.3, 5.4, 5.5 and 5.6, respectively.

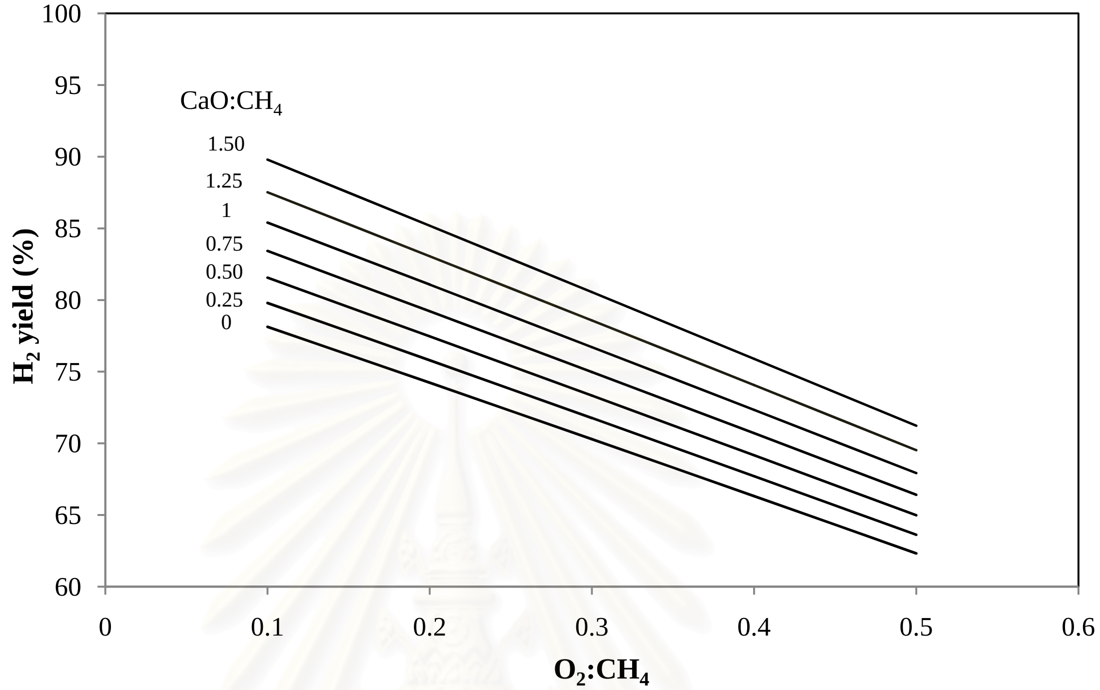

**Figure 5.3** Hydrogen yield in combined carbon dioxide reforming and partial oxidation of biogas at 973 K and $H_2O$:$CH_4$ = 5.

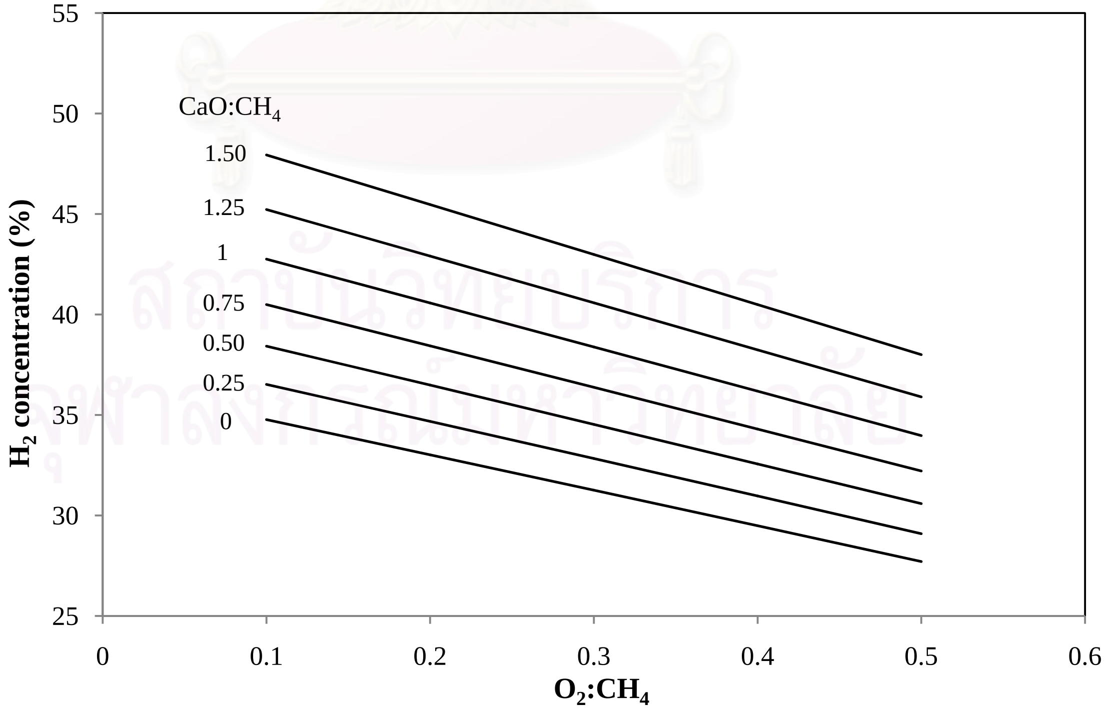

**Figure 5.4** Hydrogen concentration in combined carbon dioxide reforming and partial oxidation of biogas at 973 K and $H_2O$:$CH_4$ = 5

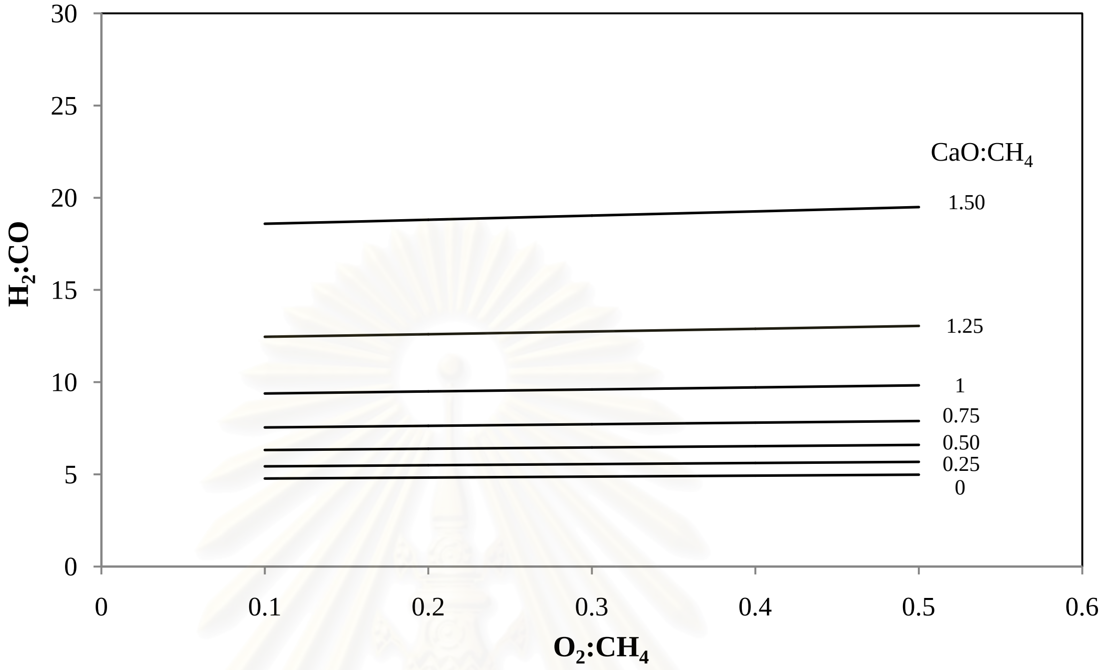

**Figure 5.5** Hydrogen: carbon monoxide ratio in combined carbon dioxide reforming and partial oxidation of biogas at 973 K and $H_2O$:$CH_4$ = 5

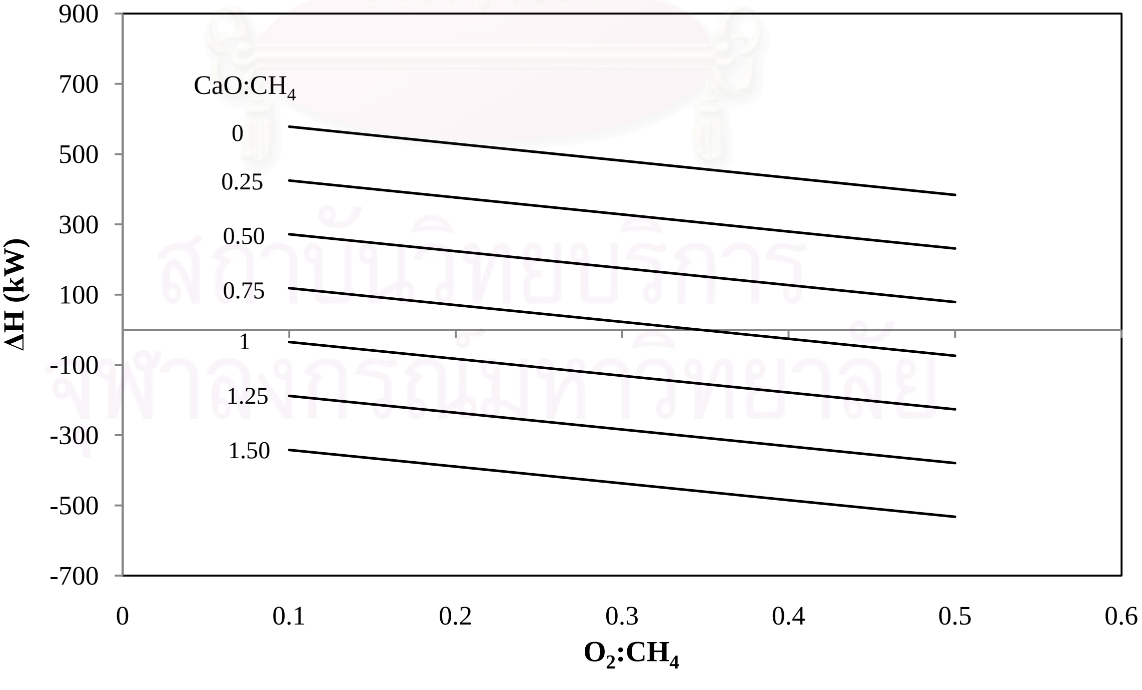

**Figure 5.6** The overall enthalpy in combined carbon dioxide reforming and partial oxidation of biogas at 973 K and $H_2O$:$CH_4$ = 5

The results show that the increasing oxygen addition decreased hydrogen yield from about 90% to below 71% at high CaO: $CH_4$ (1.5) as shown in Figure 5.3 and hydrogen concentration from about 48% to below 38% at high CaO: $CH_4$ (1.5) as shown in Figure 5.4. More oxygen content allowed the complete combustion of methane (Eq. 5.1) which contributed to the significant reduction of hydrogen yield and hydrogen concentration. Moreover, oxygen can directly react with hydrogen product to water (Eq. 5.3), resulting in the lower hydrogen product.

$$CH_4 + \tfrac{1}{2} O_2 \longrightarrow CO + 2H_2 \qquad \Delta H^\circ_{298} = -36 \text{ kJ/mol} \qquad (5.1)$$

$$CH_4 + 2O_2 \longrightarrow CO_2 + 2H_2O \qquad \Delta H^\circ_{298} = -802 \text{ kJ/mol} \qquad (5.2)$$

$$2H_2 + O_2 \longleftrightarrow 2H_2O \qquad (5.3)$$

Considering the $H_2$: CO ratio, the increasing oxygen addition affected slightly to $H_2$: CO ratio which both hydrogen and carbon monoxide concentration decreased when oxygen increased. Water generated from complete combustion and reaction with hydrogen can react with methane via steam reforming reaction. Steam reforming reaction has higher $H_2$:CO ratio so the oxygen addition contributed to more $H_2$:CO ratio. At the same CaO: $CH_4$ (1.5), $O_2$:$CH_4$ ratio from 0.1 to 0.5 gave $H_2$: CO ratios ranging from about 18.6 to 19.5 as depicted in Figure 5.5.

Furthermore, the increasing oxygen addition caused the reduction of overall enthalpy (more exothermic) because the oxygen added can react with methane via the partial oxidation (Eq. 5.2) and complete combustion. Both of reactions are exothermic, especially, the complete combustion of methane. Thus, the overall enthalpy declined extremely from about -342 to below -532 kW at high CaO: $CH_4$ (1.5) when the oxygen content increased as shown in Figure 5.6. Additionally, the CaO to methane ratio at 0.75 can occur to thermal-neutral operation (net enthalpy = 0) owing to exothermic heat from carbon dioxide sorption on CaO sorbent.

In addition, Figures 5.3 and 5.4 showed that the increasing CaO to $CH_4$ ratios from 0 to 1.5 increased hydrogen yield from a maximum value about 78% to 90% and hydrogen concentration from a maximum value about 35% to 48%. Hydrogen yield and concentration were enhanced due to the addition of CaO sorbent. Moreover, the increase of the CaO to $CH_4$ ratios from 0 to 1.5 affected $H_2$: CO ratio which increased from maximum value about 5 to 19.5 given in Figure 5.5. The CaO sorbent was added in the reaction in order to capture carbon dioxide which shifted equilibrium in water gas shift reaction (Eq. 5.5) leading to increased hydrogen product.

From the results, the use of CaO sorbent can enhance $H_2$: CO ratio, hydrogen yield and concentration and operate without requirement of external heat from other sources.

Then, the effect of the water addition on hydrogen yield, hydrogen concentration, hydrogen: carbon monoxide ratio and the overall enthalpy in the combined carbon dioxide reforming and partial oxidation of biogas was studied and the results are shown in Figures 5.7, 5.8, 5.9 and 5.10.

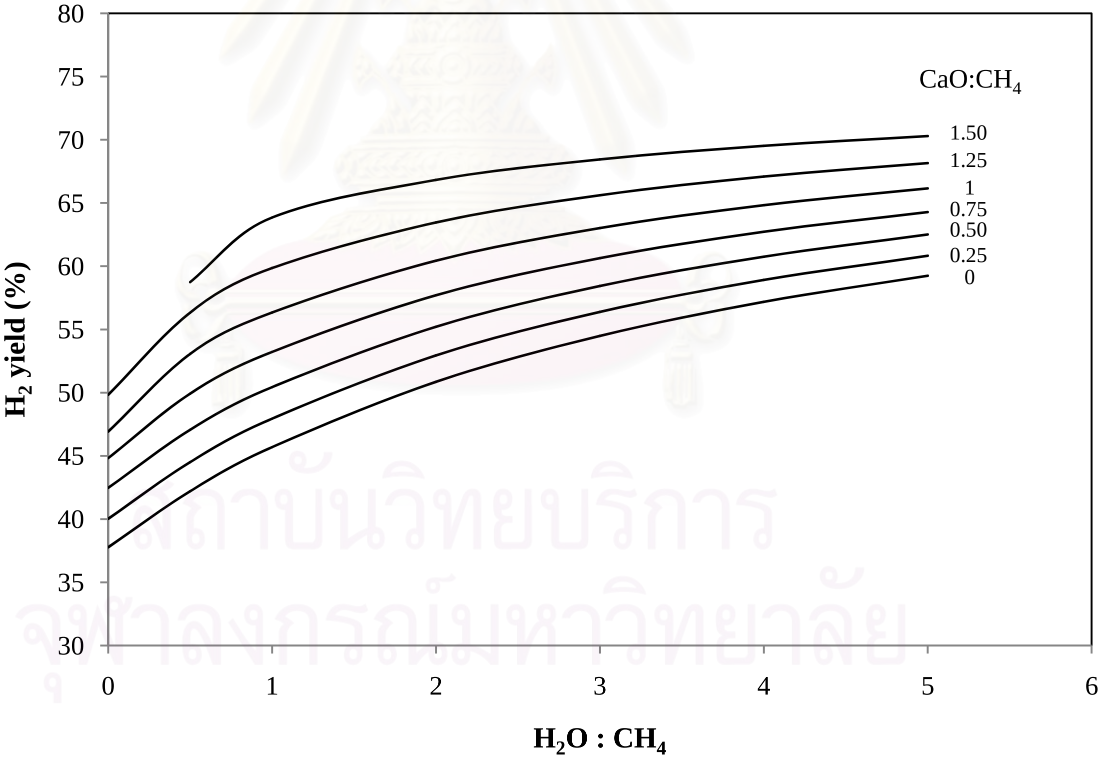

**Figure 5.7** Hydrogen yield in combined carbon dioxide reforming and partial oxidation of biogas at 1073 K and $O_2$:$CH_4$ = 0.5

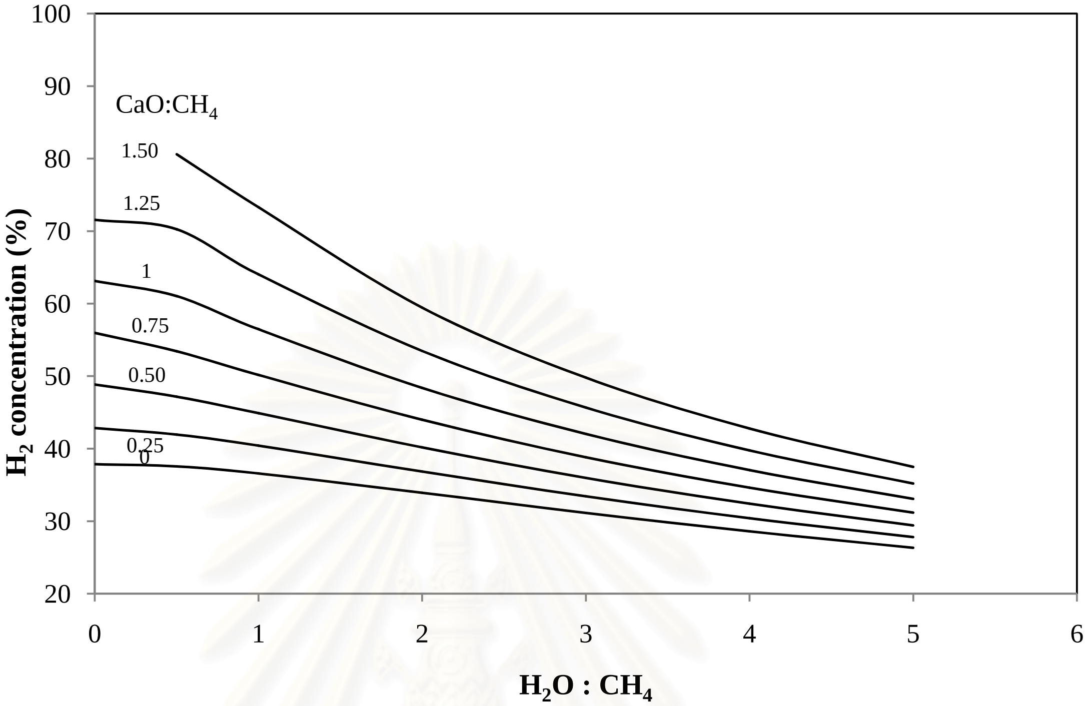

**Figure 5.8** Hydrogen concentration in combined carbon dioxide reforming and partial oxidation of biogas at 1073 K and $O_2$:$CH_4$ = 0.5

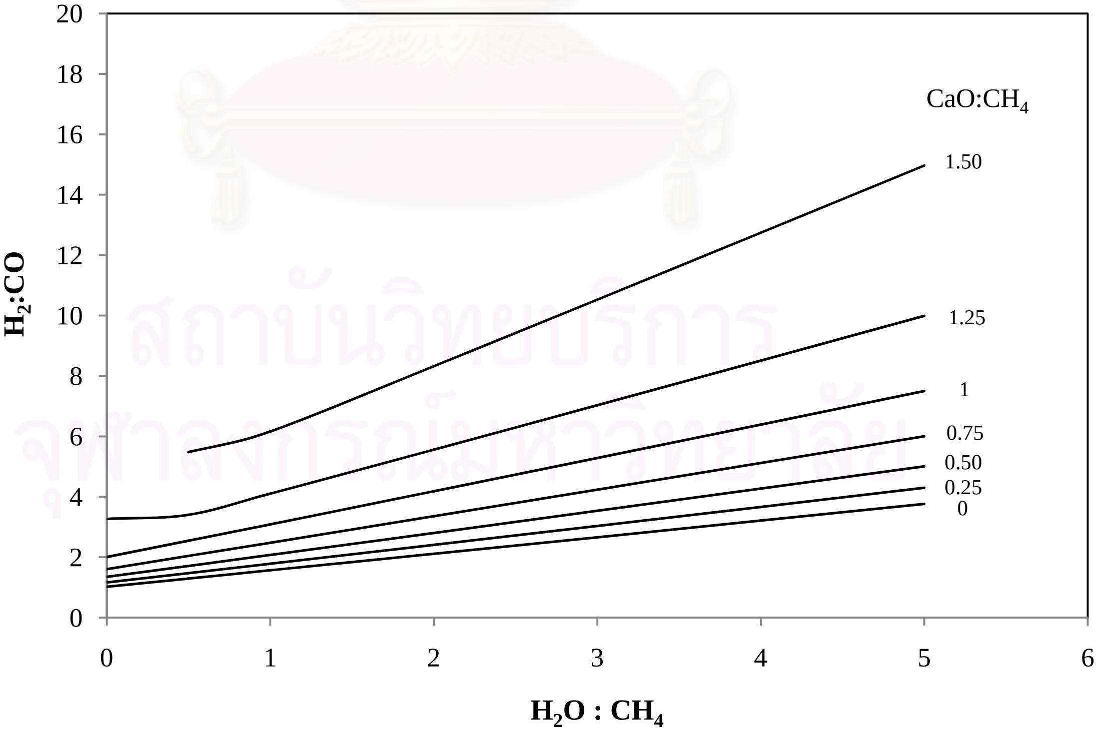

**Figure 5.9** Hydrogen: carbon monoxide ratio in combined carbon dioxide reforming and partial oxidation of biogas at 1073 K and $O_2$:$CH_4$ = 0.5

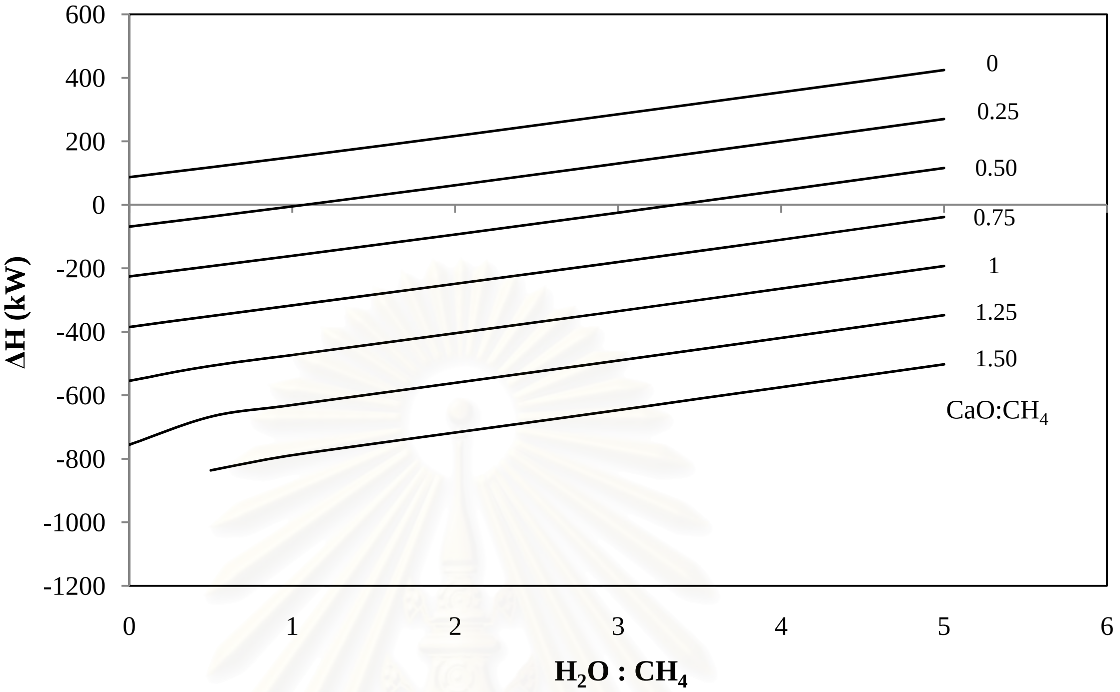

**Figure 5.10** The overall enthalpy in combined carbon dioxide reforming and partial oxidation of biogas at 1073 K and $O_2$:$CH_4$ = 0.5

The results show that the increasing water addition increased hydrogen yield from about 58 to above 70% at high CaO: $CH_4$ (1.5) as shown in Figure 5.7. More water content in the reaction caused higher hydrogen yield. This is affected by methane steam reforming (Eq. 5.4) in which methane reacted with water to hydrogen and the added water also help shift equilibrium in water gas shift reaction (Eq. 5.5). Moreover, increasing the CaO to $CH_4$ ratios from 0 to 1.5 improved hydrogen yield from maximum value about 57 to 70% as depicted in Figure 5.7. The increased CaO to $CH_4$ ratio improved hydrogen yield as the following reactions were prompted.

$$CH_4 + H_2O \longrightarrow CO + 3H_2 \qquad \Delta H^\circ_{298} = 206 \text{ kJ/mol} \qquad (5.4)$$

$$CO + H_2O \longrightarrow CO_2 + H_2 \qquad \Delta H^\circ_{298} = -40 \text{ kJ/mol} \qquad (5.5)$$

On the contrary, the increasing water addition declined hydrogen concentration from about 80 to below 37% at high CaO: $CH_4$ (1.5) as shown in Figure 5.8. More water content contributed to lower hydrogen concentration because water diluted product. Considering the effect of CaO addition of CaO, more CaO addition increased hydrogen concentration. From Figure 5.8, the maximum CaO to $CH_4$ ratios (1.5) gave hydrogen concentration which increased up to 10% compared with no CaO sorbent.

From Figure 5.9, the increasing water addition increased hydrogen to carbon monoxide ratio from about 5.48 to 14.96 at high CaO: $CH_4$ (1.5) because the water addition allowed the methane steam reforming to take place with a hydrogen to carbon monoxide ratio of 3. Additionally, the addition of CaO caused increasing $H_2$: CO ratio from about 3.77 to 14.96 at constant $H_2O$: $CH_4$ (5).

Besides, the overall enthalpy increased greatly from about -836 to above -502 kW at high CaO: $CH_4$ (1.5) when the water content increased which was given in Figure 5.10. Both of reactions are endothermic. Especially, the methane steam reforming of is highly endothermic; the overall enthalpy in reaction becomes more endothermic.

From the combined carbon dioxide reforming and partial oxidation of biogas at 1073 K and $O_2$:$CH_4$ = 0.5, the self- sustained heat can take place at the CaO to $CH_4$ ratios equal 0.25 and 0.5 as shown in Figure 5.10.

After that, the effect of the CaO addition on hydrogen yield, hydrogen concentration, hydrogen: carbon monoxide ratio and the overall enthalpy in the combined carbon dioxide reforming and partial oxidation of biogas was investigated and depicted in Figures 5.11, 5.12, 5.13 and 5.14.

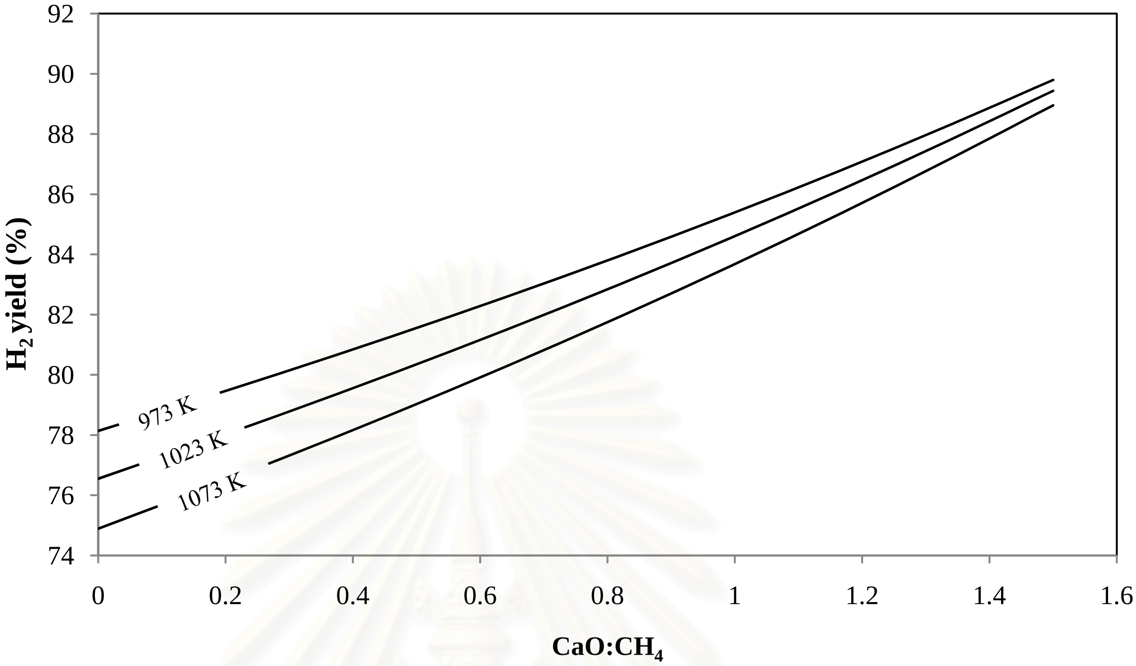

**Figure 5.11** Hydrogen yield in combined carbon dioxide reforming and partial oxidation of biogas at $O_2$:$CH_4$ = 0.1 and $H_2O$:$CH_4$ = 5

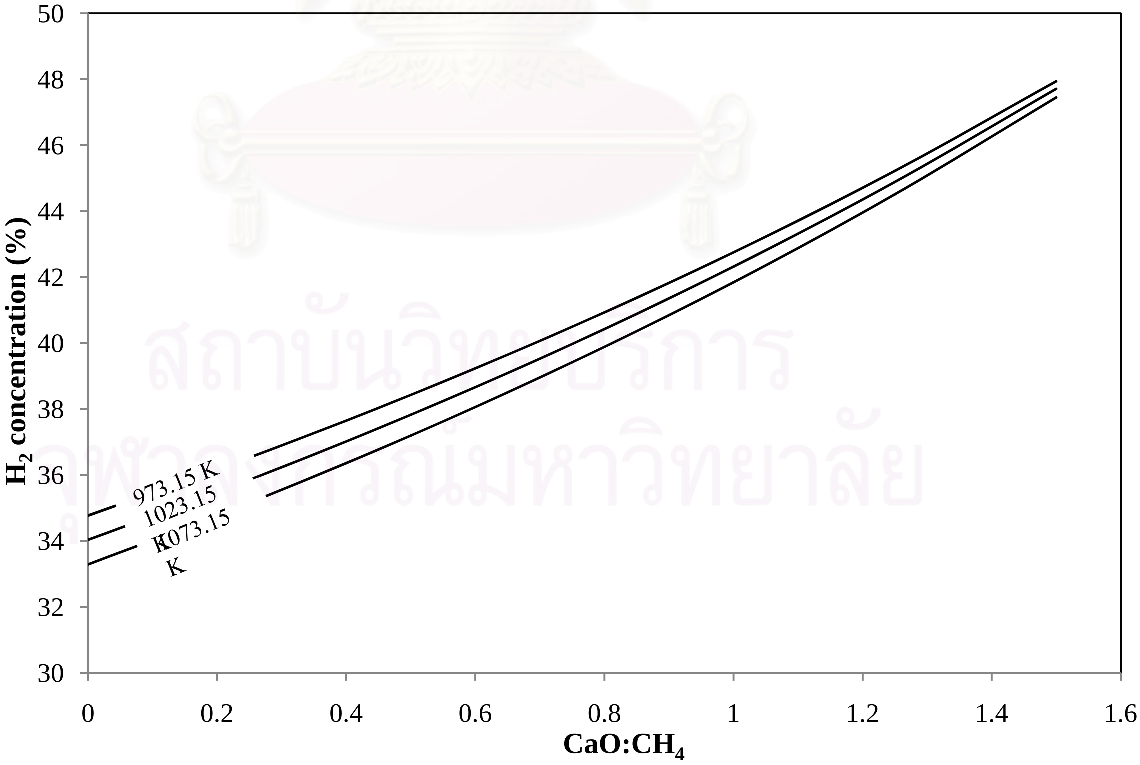

**Figure 5.12** Hydrogen concentration in combined carbon dioxide reforming and partial oxidation of biogas at $O_2$:$CH_4$ = 0.1 and $H_2O$:$CH_4$ = 5

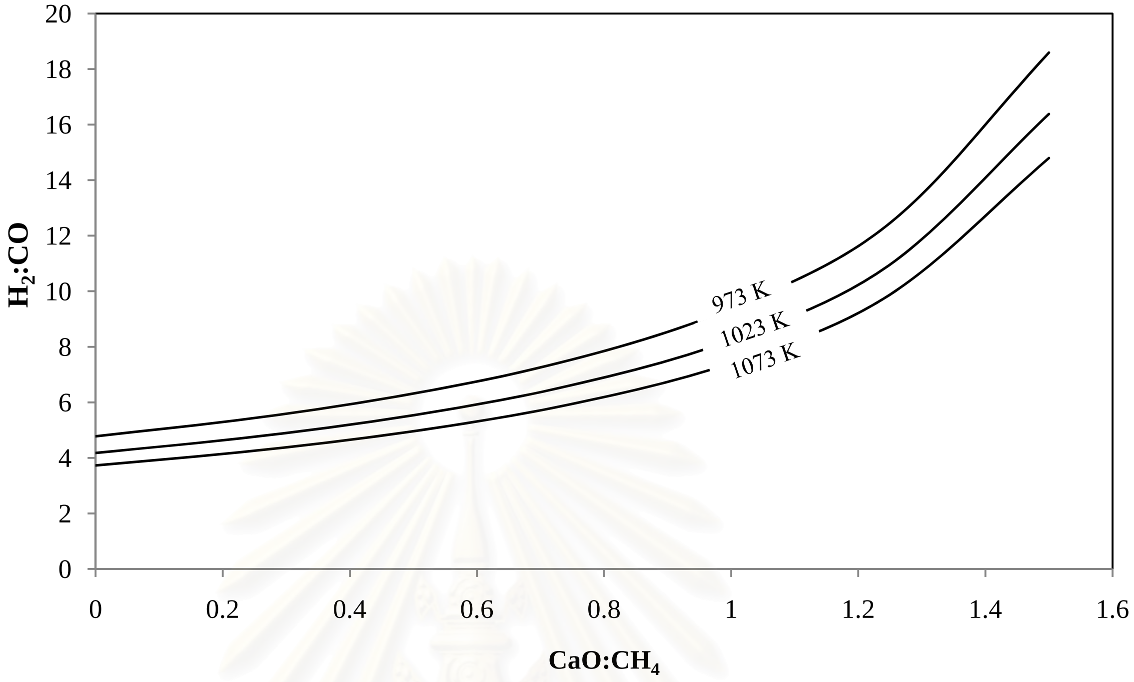

**Figure 5.13** Hydrogen: carbon monoxide ratio in combined carbon dioxide reforming and partial oxidation of biogas at $O_2$:$CH_4$ = 0.1 and $H_2O$:$CH_4$ = 5

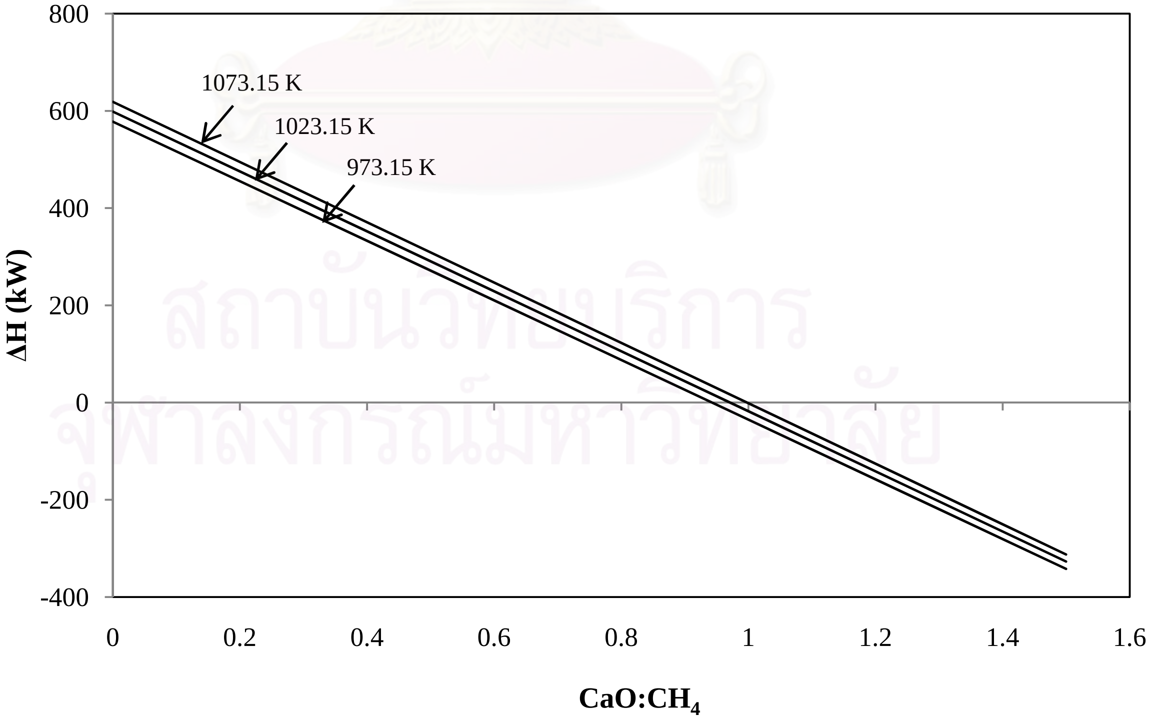

**Figure 5.14** The overall enthalpy in combined carbon dioxide reforming and partial oxidation of biogas at $O_2$:$CH_4$ = 0.1 and $H_2O$:$CH_4$ = 5

The results indicate that the increasing CaO increased hydrogen yield from about 78 to above 90% at low temperature (973 K) as shown in Figure 5.11 and hydrogen concentration from about 35% to above 48% at low temperature (973 K) as shown in Figure 5.12. More CaO sorbent in the reaction produced higher hydrogen yield. From Figure 5.13, the addition of CaO sorbent also increased $H_2$: CO ratio from 4.78 to 18.59 at low temperature (973 K). Because CaO adsorbed carbon dioxide, water gas shift reaction (Eq. 5.5) is equilibrium shifted, resulting in higher hydrogen product. The CaO sorbent was able to enhance hydrogen to carbon monoxide ratio, hydrogen yield and concentration.

On the contrary, the CaO addition decreased considerably the overall enthalpy from about 578 to below -342 kW at low temperature (973 K) which was given in Figure 5.14. This is affected by carbonation reaction (Eq. 5.6) in which CaO adsorbed carbon dioxide to calcium carbonate ($CaCO_3$). The carbonation reaction is greatly exothermic so more CaO addition contributed to more exothermic.

$$CaO + CO_2 \longrightarrow CaCO_3 \qquad \Delta H^\circ_{298} = -178\ \text{kJ/mol} \qquad (5.6)$$

Finally, the effect of temperature on hydrogen yield, hydrogen concentration, hydrogen: carbon monoxide ratio and the overall enthalpy in the combined carbon dioxide reforming and partial oxidation of biogas were shown in Figures 5.11, 5.12, 5.13 and 5.14.

From Figure 5.11, the hydrogen yield tended to decline slightly with increasing reaction temperature from maximum value about 90% at high temperature (1073 K) to 89% at low temperature (973 K). For hydrogen concentration, it decreased slightly when the reaction temperature was higher from a maximum value about 47.9% at high temperature (1073 K) to 47.7% at low temperature (973 K). In addition, the hydrogen to carbon monoxide ratio also declined from maximum value about 14.8 at high temperature (1073 K) to 18.59 at low temperature (973 K). This is because the exothermic reactions are clearly preferred at low temperature. Exothermic reactions such as partial oxidation of methane (Eq. 5.1) and water gas shift reaction (Eq. 5.5) caused higher hydrogen to carbon monoxide ratio, hydrogen yield and concentration.

On the contrary, the overall enthalpy increased slightly from about 578 to 610 kW when the reaction temperature increased from 973 to 1073 K as given in Figure 5.14. This is caused by exothermic reactions which favored at low temperature. Thus, low temperature showed slightly higher exothermicity than high temperature in this reaction. Furthermore, the reaction temperatures at 973, 1023 and 1073 K can offer thermal-neutral operation by adjusting a suitable amount of CaO sorbent.

## 5.3 The thermal-neutral operation

This part focused on the thermal-neutral operation (net enthalpy = 0) of the combined carbon dioxide reforming and partial oxidation of biogas. Under this condition, heat from exothermic reaction was used for supplying energy required for endothermic reaction at equivalent amount, so that this system did not rely on external heat source. For the thermal-neutral operation, oxygen to methane ratio, hydrogen yield, hydrogen concentration and hydrogen to carbon dioxide ratio at various temperatures (973, 1023 and 1073 K) were shown in Figures 5.15-5.26.

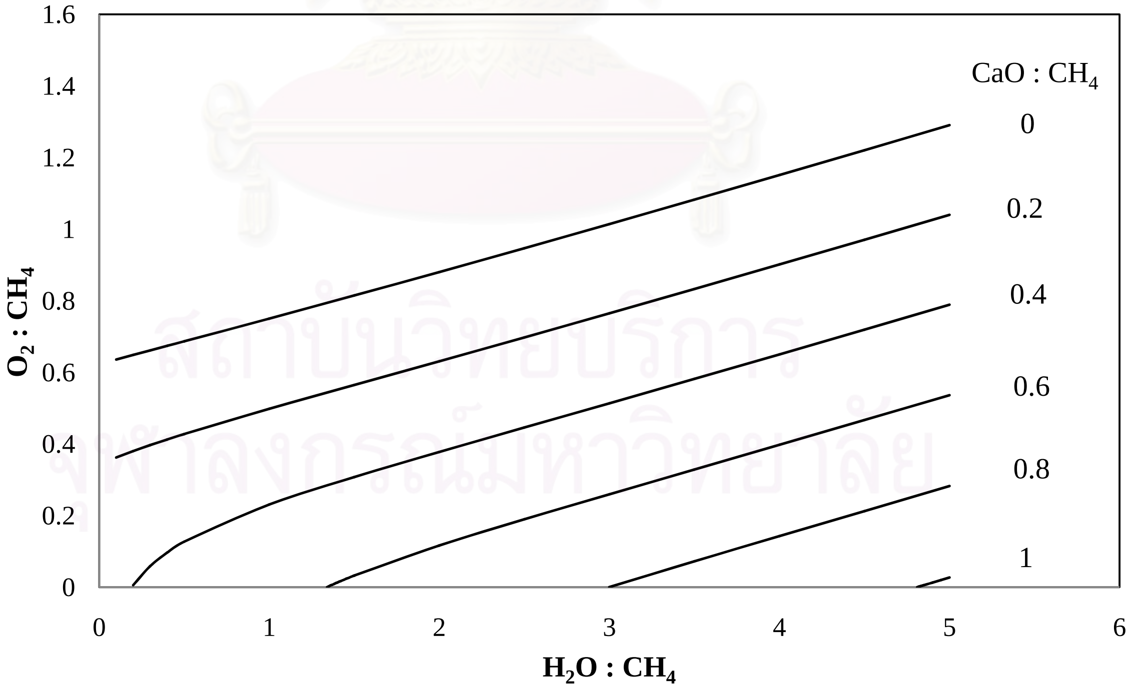

**Figure 5.15** Oxygen to methane ratio in combined carbon dioxide reforming and partial oxidation of biogas at ΔH= 0 and 973 K

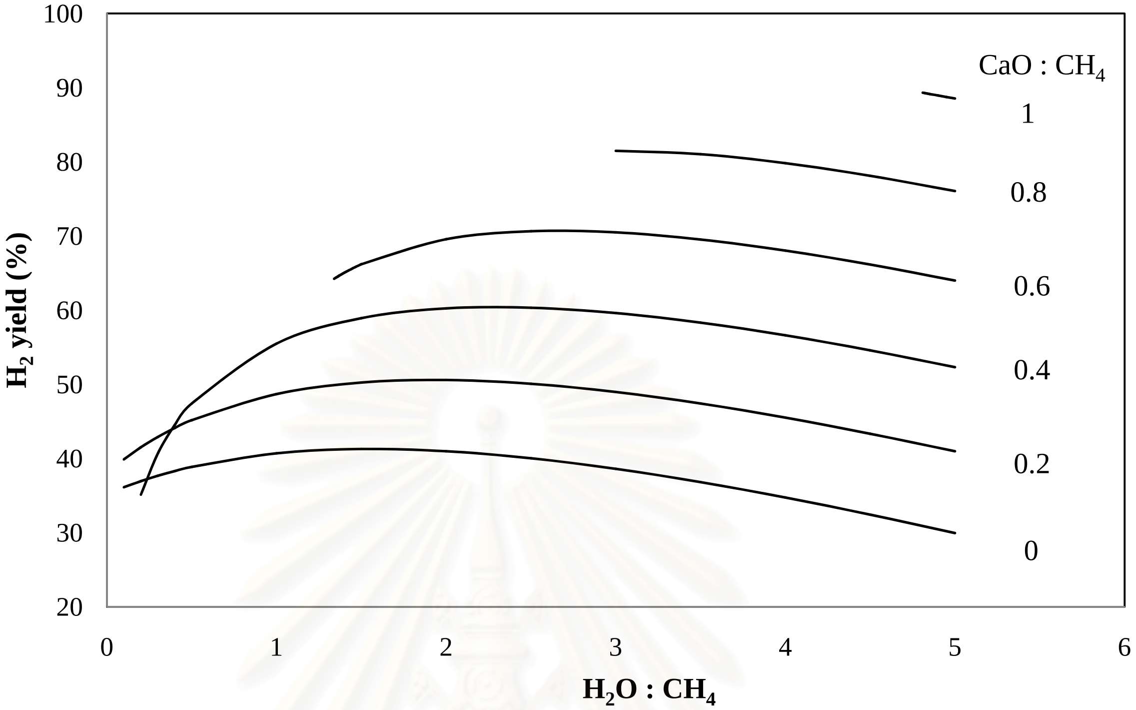

**Figure 5.16** Hydrogen yield in combined carbon dioxide reforming and partial oxidation of biogas at ΔH= 0 and 973 K

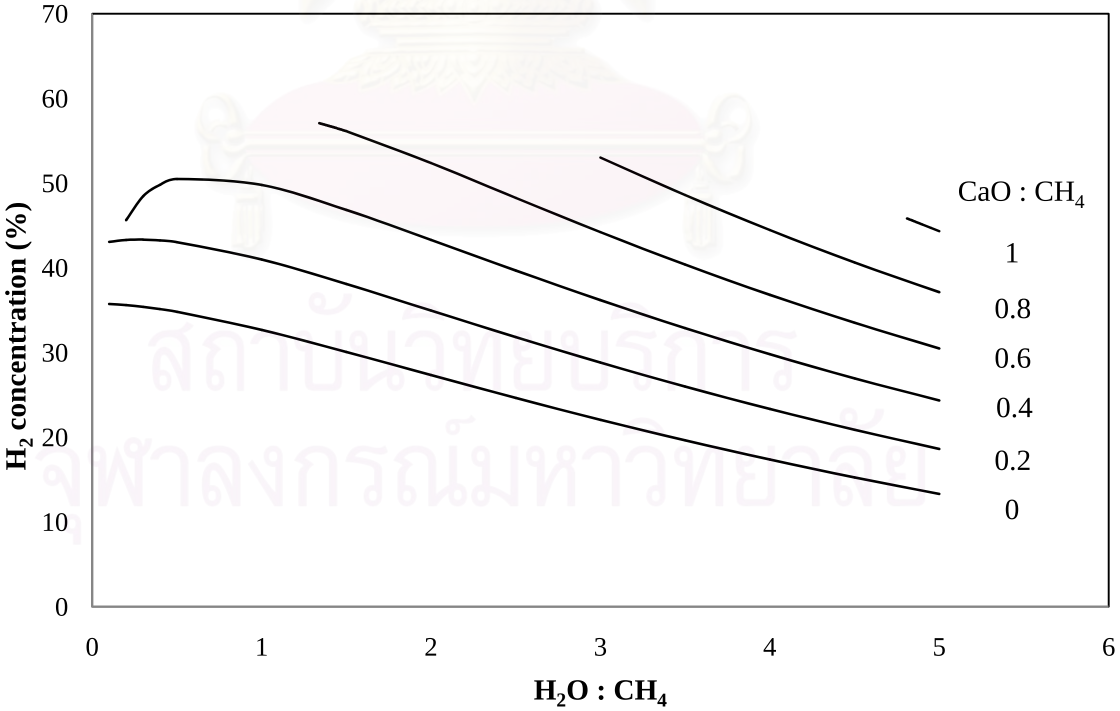

**Figure 5.17** Hydrogen concentration in combined carbon dioxide reforming and partial oxidation of biogas at ΔH= 0 and 973 K

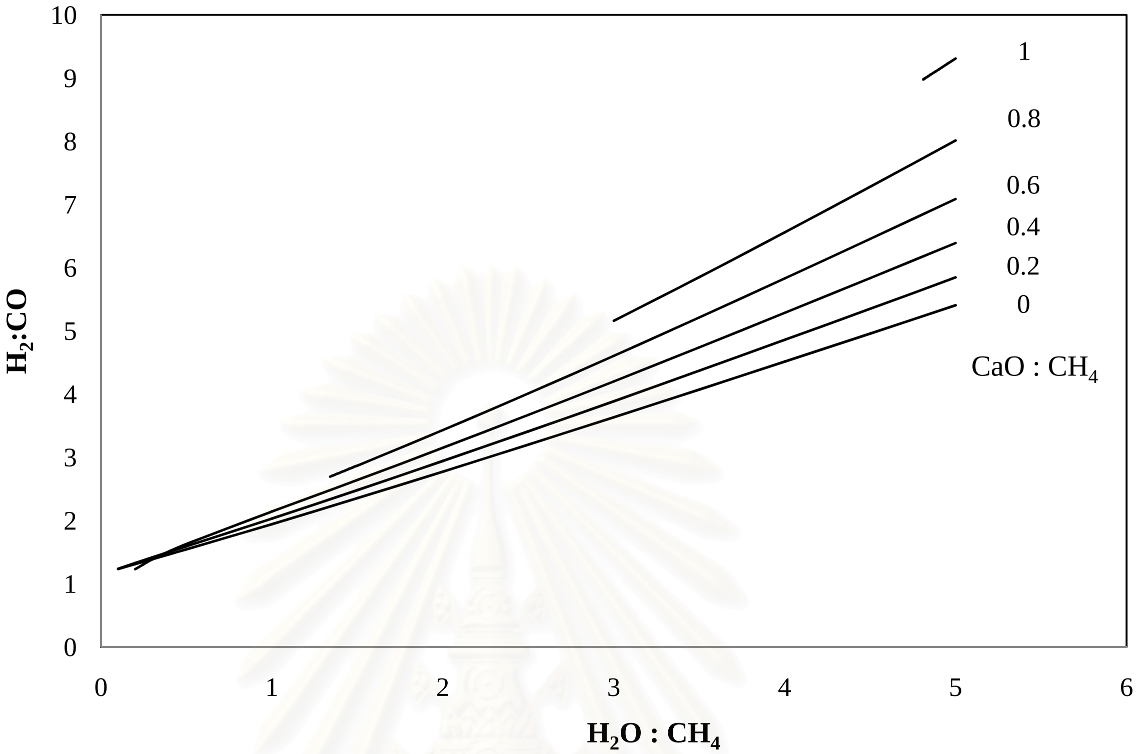

**Figure 5.18** Hydrogen to carbon monoxide ratio in combined carbon dioxide reforming and partial oxidation of biogas at ΔH= 0 and 973 K

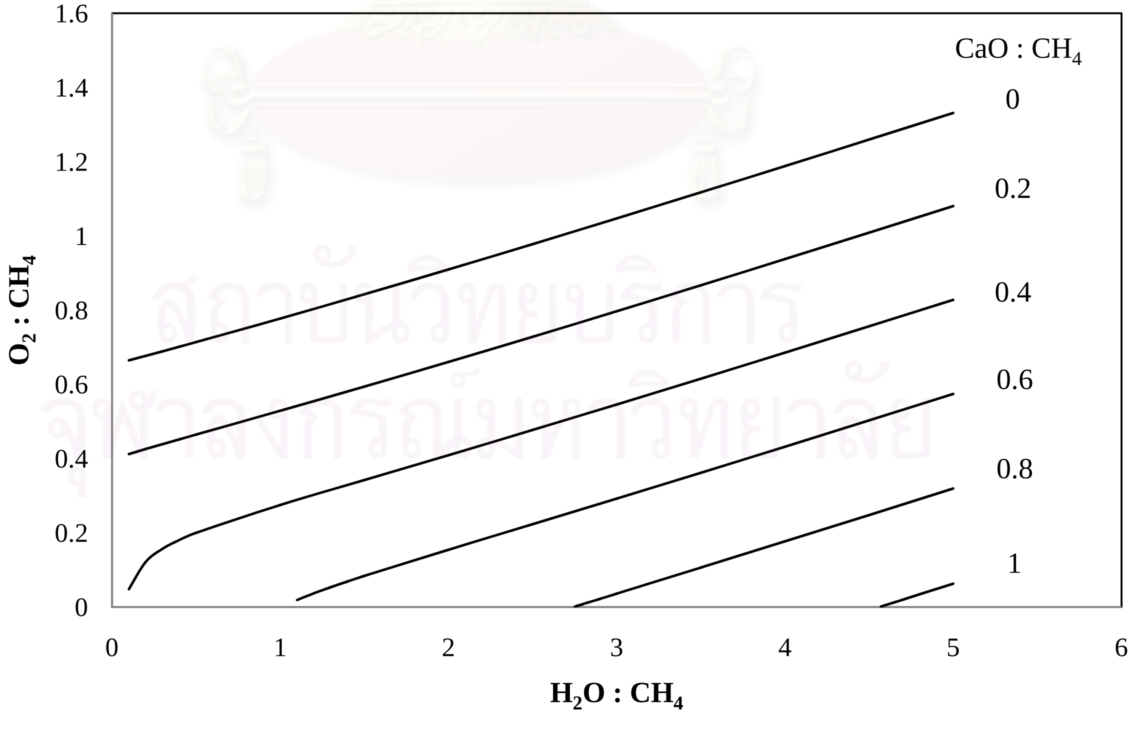

**Figure 5.19** Oxygen to methane ratio in combined carbon dioxide reforming and partial oxidation of biogas at ΔH= 0 and 1023 K

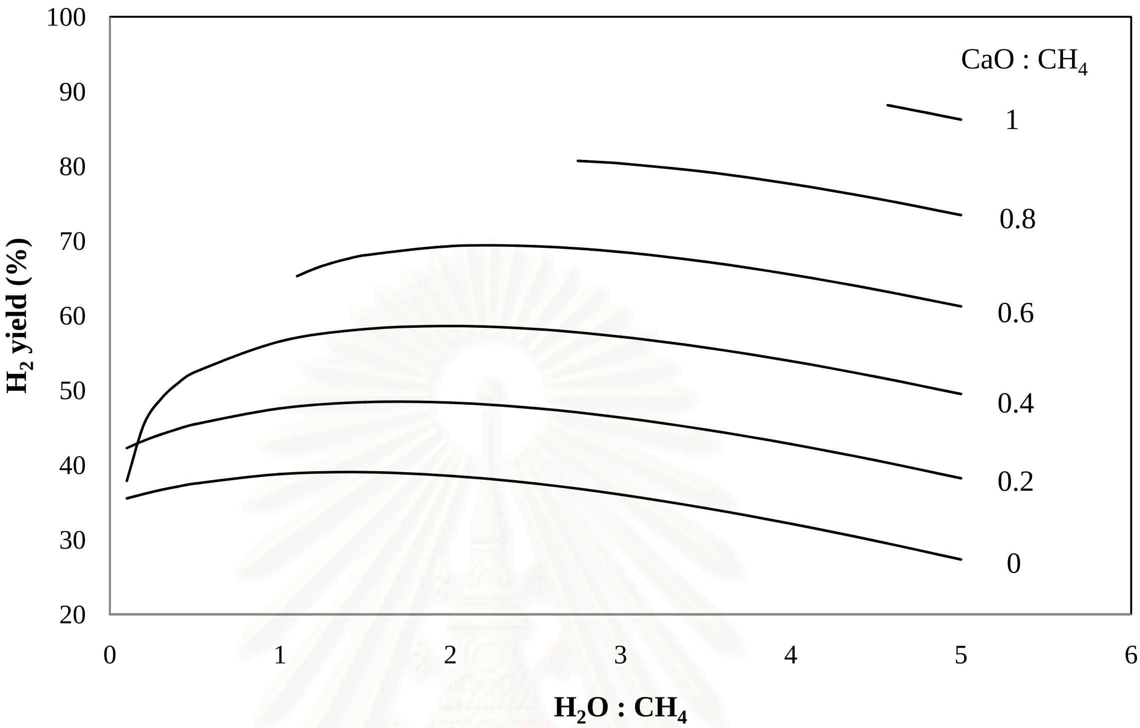

**Figure 5.20** Hydrogen yield in combined carbon dioxide reforming and partial oxidation of biogas at ΔH= 0 and 1023 K

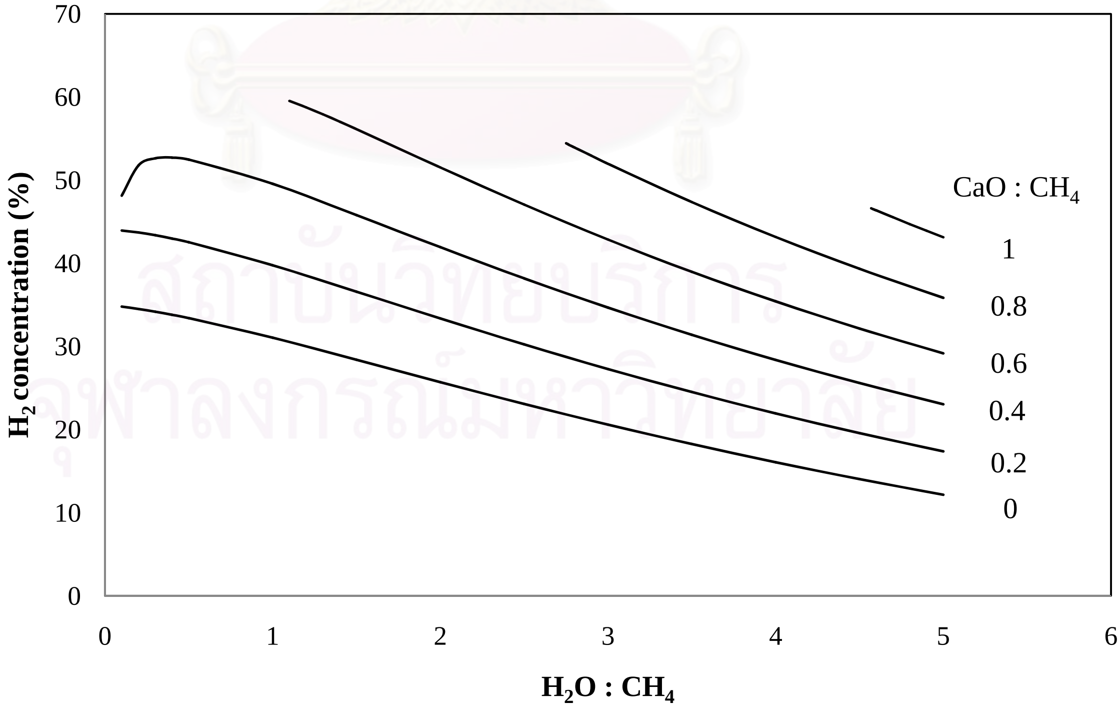

**Figure 5.21** Hydrogen concentration in combined carbon dioxide reforming and partial oxidation of biogas at ΔH= 0 and 1023 K

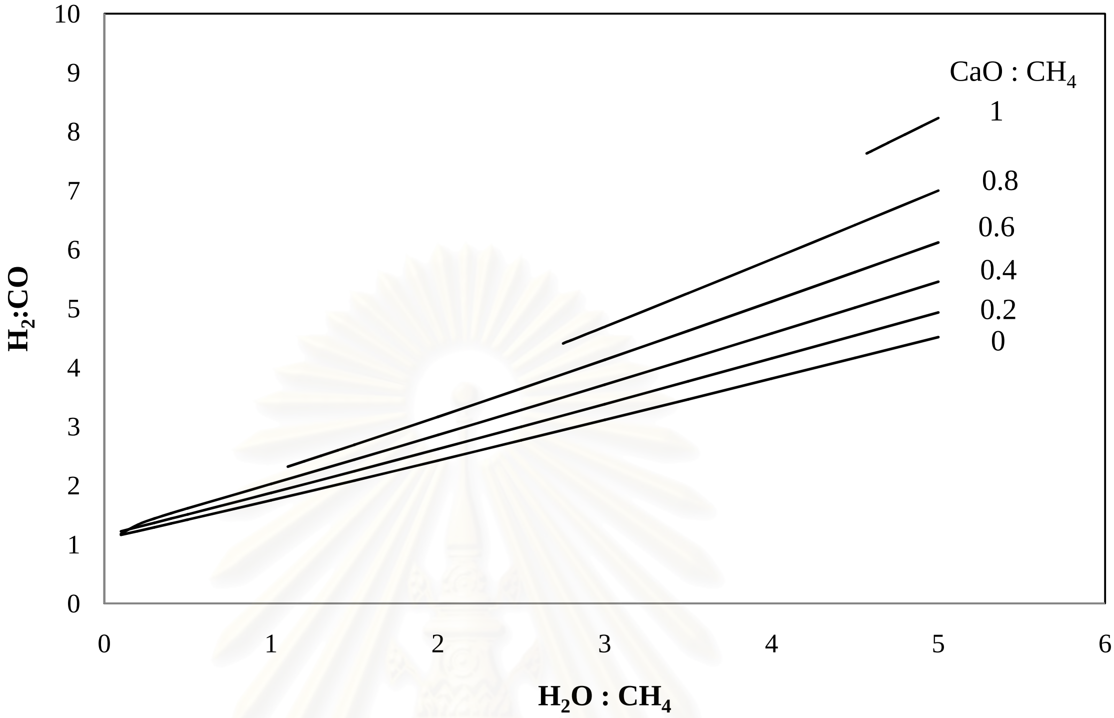

**Figure 5.22** Hydrogen to carbon monoxide ratio in combined carbon dioxide reforming and partial oxidation of biogas at ΔH= 0 and 1023 K

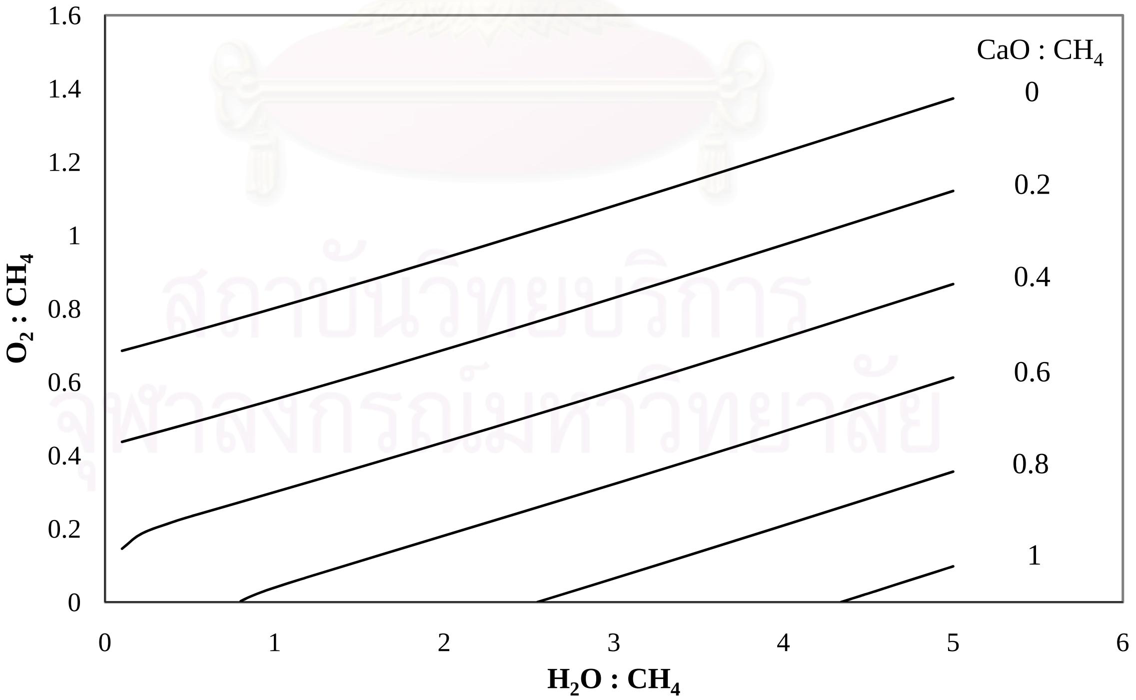

**Figure 5.23** Oxygen to methane ratio in combined carbon dioxide reforming and partial oxidation of biogas at ΔH= 0 and 1073 K

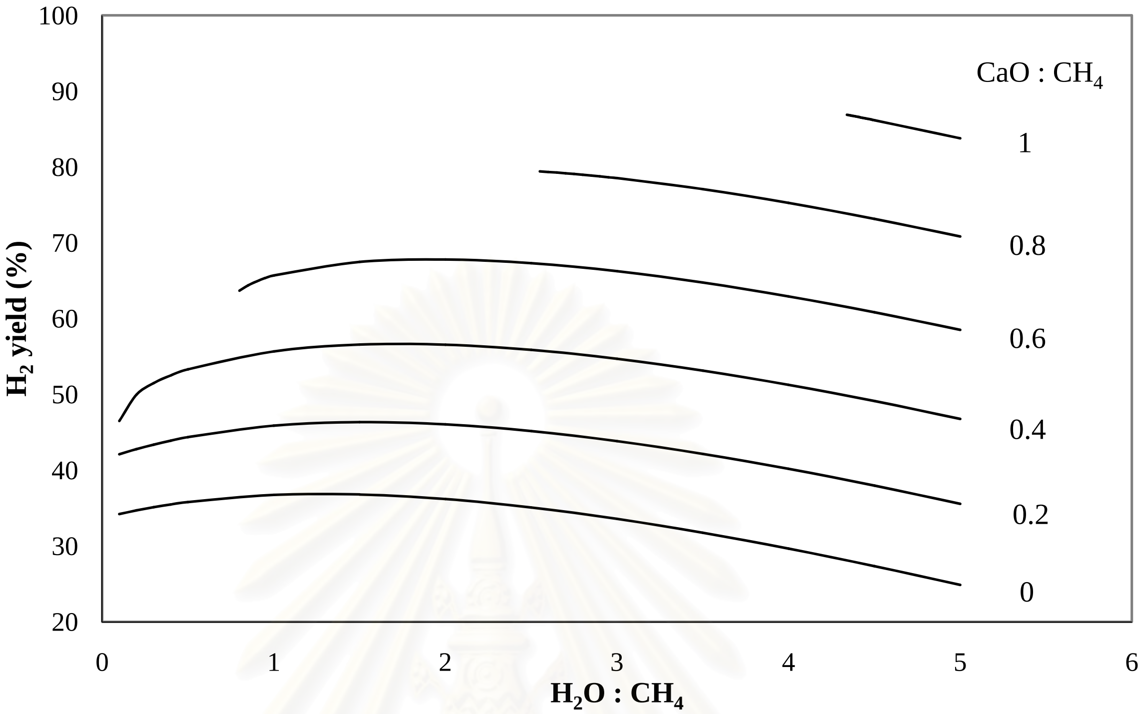

**Figure 5.24** Hydrogen yield in combined carbon dioxide reforming and partial oxidation of biogas at ΔH= 0 and 1073 K

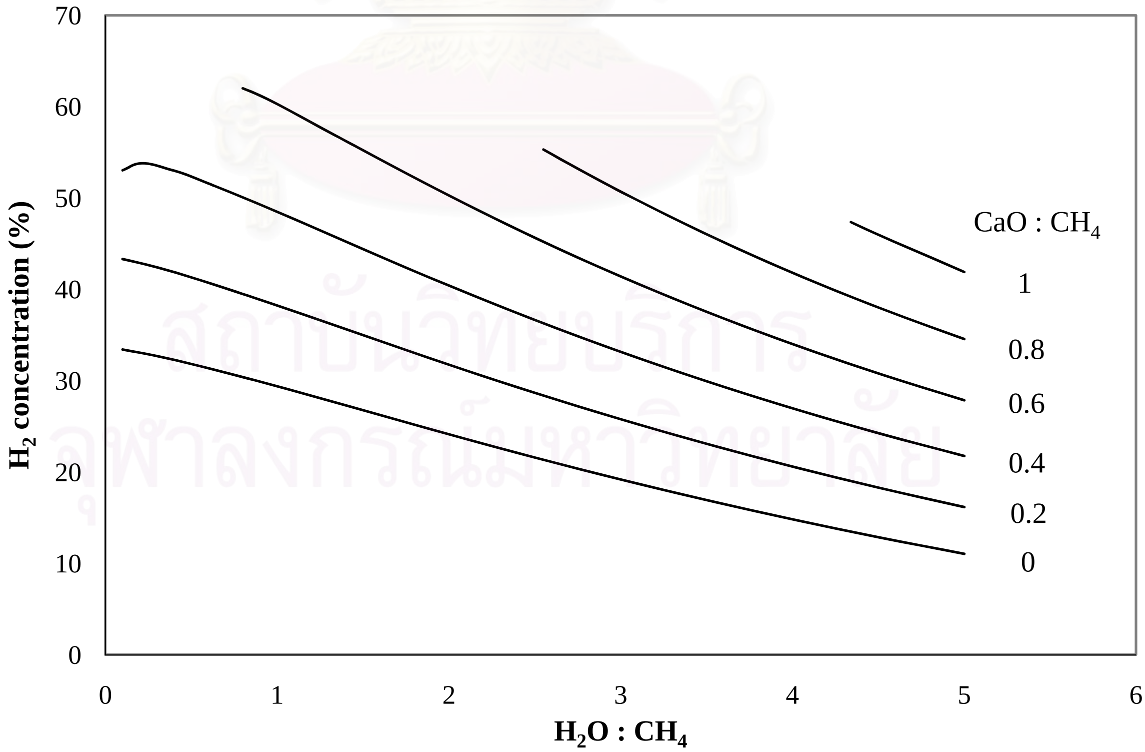

**Figure 5.25** Hydrogen concentration in combined carbon dioxide reforming and partial oxidation of biogas at ΔH= 0 and 1073 K

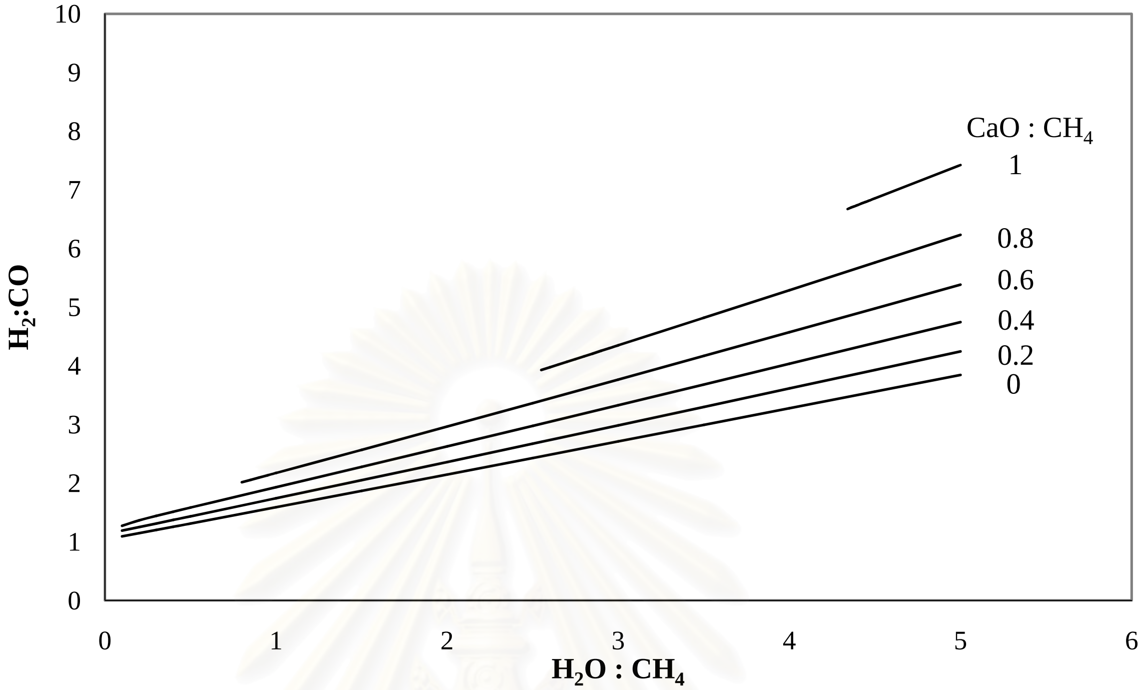

**Figure 5.26** Hydrogen to carbon monoxide ratio in combined carbon dioxide reforming and partial oxidation of biogas at ΔH= 0 and 1073 K

From the results of the combined carbon dioxide reforming and partial oxidation of biogas at the overall enthalpy equal zero were shown in Figures 5.15-26 indicating results of $O_2$:$CH_4$ ratio, hydrogen yield, hydrogen concentration and hydrogen to carbon monoxide ratio at various temperatures (973, 1023 and 1073 K).

At the same CaO:$CH_4$ ratio, the $O_2$:$CH_4$ ratio required for feeding into the reaction increased when the water addition increased to allow the thermal-neutral operation. From Figure 5.15, the increasing water content from 0.1 to 5 at no CaO contributed to the increasing $O_2$:$CH_4$ ratio from about 0.64 to 1.3 in order to make self-sustained heat. The addition water tended to enhance endothermic reaction and, therefore, more oxygen was required to increase exothermic reaction to achieve a thermal neutral condition.

On the contrary, the increase of CaO: $CH_4$ ratio from 0 to 1 required the use of lower $O_2$:$CH_4$ ratio; i.e., the maximum value decreased from 1.3 to 0.02 when the $H_2O$:$CH_4$ ratio was kept at 5 as shown in Figure 5.15. The addition of CaO contributed to carbonation, which is highly exothermic so amount of oxygen in reaction decreased in order to reduce excessive exothermic heat to be equivalent to the endothermic heat.

The results presented in Figure 5.16 indicated that operation at CaO:$CH_4$ = 1, $H_2O$:$CH_4$ = 4.8 and $O_2$:$CH_4$ = 0.00013 resulted in maximum hydrogen yield which was 89.3% when $H_2O$:$CH_4$ increased to 5, leading to lower hydrogen yield (88.7%). Moreover, the CaO addition increased hydrogen yield due to carbon dioxide sorption and shifting of water gas shift reaction (Eq. 5.5). The CaO:CH4 ratio at 0.6, 0.4, 0.2 and 0 had maximum points of hydrogen yield at 70.6, 60.3, 50.6 and 41.3%, respectively.

In view of hydrogen concentration given in Figure 5.17, more water addition declined hydrogen concentration at the constant CaO:$CH_4$ ratio. In contrast, more CaO addition enhanced hydrogen concentration which tended similar hydrogen yield.

Furthermore, the addition of water increased the hydrogen to carbon monoxide ratio owing to methane steam reforming which occurred high $H_2$:CO. The addition of CaO sorbent also improved the hydrogen to carbon monoxide ratio as shown in Figure 5.18.

Considering the effect of temperature, the oxygen addition in order to make thermal-neutral operation at high temperature was higher than low temperature compared in Figures 5.15, 5.19 and 5.23. Because endothermic reactions favored at high temperature, the increasing oxygen content in this reaction in order to give enough exothermic heat equaled endothermic heat.

The effect of temperature on hydrogen yield in thermal-neutral operation was showed in Figures 5.16, 5.20 and 5.24. These indicated that the maximum hydrogen yield of each CaO:$CH_4$ ratio declined slightly when the temperature increased. This result tended similarly Figure 5.11 which hydrogen yield at high temperature lower than low temperature.

In contrast, the maximum hydrogen concentration of each CaO:$CH_4$ ratio increased when the temperature raised which the effect of temperature was showed in

Figures 5.17, 5.21 and 5.25. Because of the lower water addition at high temperature, the diluting water content was low contributed to more hydrogen concentration.

Finally, The effect of temperature on hydrogen to carbon monoxide ratio in thermal-neutral operation was showed in Figures 5.18, 5.22 and 5.26. These indicated that the hydrogen to carbon monoxide ratio of each CaO:$CH_4$ ratio declined slightly when the temperature increased. The trend is similarly to that of Figure 5.13.

# CHAPTER VI

# CONCLUSIONS AND RECOMMENDATIONS

This chapter is divided into two sections. In the first section, the conclusions gained from the experimental studies on the effect of adsorbent and catalyst bed arrangement on the combined carbon dioxide reforming and partial oxidation of biogas from the simulation studies on the effects of temperature, oxygen, water and CaO sorbent on the combined carbon dioxide reforming and partial oxidation of biogas particularly under thermal-neutral operation are summarized in this section. The recommendations for further study are given in the other section.

## 6.1 Conclusions

1. From the experimental study, the use of CaO in the combined carbon dioxide reforming and partial oxidation of biogas especially for the mode of mixture of CaO and Ni/$SiO_2$.MgO can enhance the hydrogen yield over the conventional system. The improved hydrogen yield was observed until 80 minutes of reaction time.

2. From the simulation study, the increasing oxygen into the combined carbon dioxide reforming and partial oxidation of biogas decreased hydrogen yield and concentration but it increased exothermic heat. In addition, more oxygen in feed decreased slightly the hydrogen to carbon monoxide ratio. The $O_2$:$CH_4$ ratio which gives optimum hydrogen yield is 0.1.

3. The addition of water into the combined carbon dioxide reforming and partial oxidation of biogas was able to enhance hydrogen yield and hydrogen to carbon monoxide ratio. In view of hydrogen concentration, it was found that the water addition caused the decrease of hydrogen concentration. Furthermore, the addition of water was contributed to higher endothermic heat.

4. The CaO addition into the combined carbon dioxide reforming and partial oxidation of biogas in order to absorb carbon dioxide can improve hydrogen to carbon

monoxide ratio, hydrogen yield and concentration. The $CO_2$ sorption reaction can also supply the exothermic heat for the reaction system.

5. At higher operating temperature, the hydrogen to carbon monoxide ratio, hydrogen yield and concentration decreased. In contrast, the overall enthalpy increased at high temperature. An optimum operating temperature for the combined carbon dioxide reforming and partial oxidation of biogas was at 973 K.

6. The combined carbon dioxide reforming and partial oxidation of biogas can operate at various conditions in order to occur with thermal-neutral operation. From the result, the condition which gives an optimum hydrogen yield of 89.3% with $H_2$: CO = 8.98 are $O_2$:$CH_4$ = 0.00013, $H_2O$:$CH_4$ = 4.8 and CaO: $CH_4$ = 1 at 973 K.

## 6.2 Recommendations

1. More experiments should be carried out particularly for the combined carbon dioxide reforming and partial oxidation of biogas with co feed of water in order to enhance hydrogen yield. In addition, this reaction should be performed using wider ranges of the manipulated variables such as $O_2$:$CH_4$, $CO_2$:$CH_4$, $H_2O$:$CH_4$, CaO:$CH_4$ ratios and reaction temperature.

2. CaO used in the combined carbon dioxide reforming and partial oxidation of biogas should be characterized in order to investigate surface area.

3. The results of simulation should be verified with experimental results. For this work the equilibrium-based model was employed as the preliminary studies. It is advisable to develop a more rigorous mathematical model taking into account reaction kinetics so that the simulation results become more realistic.

# REFERNCES

Abanades, J. C. The maximum capture efficiency of $CO_2$ using carbonation/calcinations cycle of $CaO/CaCO_3$. Chemical Engineering Journal 90 (2002): 303-306.

Alstrup, I. A new model explaining carbon filament growth on nickel, iron, and Ni-Cu alloy catalysts. Journal of Catalysis 109 (1988): 241-251.

Balasubramanian, B., Ortiz, A.L., Kaytakoglu, S. and Harrison, D.P. Hydrogen from methane in a single-step process. Chemical Engineering Science 54 (1999): 3543–3552.

Barelli, L., Bidini, G., Gallorini, F. and Servili, S. Hydrogen production through sorption-enhanced steam methane reforming and membrane technology: A review. Energy 33 (2008): 554–570.

Charoenseri, S. Combined carbon dioxide reforming and partial oxidation of methane under periodic operation. Master Degree Chemical Engineering Faculty of Engineering Chulalongkorn University, 2007.

Choudhary, V. R. and Mamman, A. S. Energy efficient conversion of methane to syngas over NiO–MgO solid solution. Applied Energy 66 (2000): 161-175.

Dasgupta, D., Mondal, K. and Wiltowski, T. Robust, high reactivity and enhanced capacity carbon dioxide removal agents for hydrogen production applications. International Journal of Hydrogen Energy 33 (2008): 303 – 311.

Erdöhelyi, A., Cserényi, J., Papp, E. and Solymosi, F. Catalytic reaction of methane with carbon dioxide over supported palladium. Applied Catalysis A: General 108 (1994): 205-219.

Ermakova, M. A., and Ermakov, D. Y. $Ni/SiO_2$ and $Fe/SiO_2$ catalysts for production of hydrogen and filamentous carbon via methane decomposition. Catalysis Today 77 (2002): 225-235.

Freni, S., Calogero, G. and Cavallaro, S. Hydrogen production from methane through catalytic partial oxidation reactions. Journal of Power Sources 87 (2000): 28–38.

Gupta, H and Fan, L.S. Carbonation-Calcination Cycle Using High Reactivity Calcium Oxide for Carbon Dioxide Separation from Flue Gas. Industrial & Engineering Chemistry Research 41 (2002): 4035-4042.

Halmann, M. and Steinfeld, A. Production of lime, hydrogen, and methanol by the thermo-neutral combined calcination of limestone with partial oxidation of natural gas or coal. Energy 31 (2006): 1533–1541.

Han, C. and Harrison, D.P. Simultaneous shift reaction and carbon dioxide separation for the direct production of hydrogen. Chemical Engineering Science 49 (1994): 5875–5883.

Ito, M., Tagawa, T., and Goto, S. Suppression of carbonaceous depositions on nickel catalyst for the carbon dioxide reforming of methane. Applied Catalysis A: General 177 (1999): 15-23.

Japan Petroleum Energy Center. http://www.pecj.or.jp/japanese/report/report02/report-pdf/99surv7-e.pdf. Japan, 1999.

Jing, Q., Lou, H., Fei, J., Hou, Z., and Zheng, X. Syngas production from reforming of methane with $CO_2$ and $O_2$ over Ni/SrO-$SiO_2$ catalysts in a fluidized bed reactor. International Journal of Hydrogen Energy 29 (2004): 1245-1251.

Jing, Q. S., Fei, J. H., Lou, H., Mo, L. Y., and Zheng, X. M. Effective reforming of methane with $CO_2$ and $O_2$ to low $H_2$/CO ratio syngas over Ni/MgO-$SiO_2$ using fluidized bed reactor. Energy Conversion and Management 45 (2004): 3127-3137.

Jing, Q., Lou, H., Mo, L., and Zheng, X. Comparative study between fluidized bed and fixed bed reactors in methane reforming with $CO_2$ and $O_2$ to produce syngas. Energy Conversion and Management 47 (2006): 459-469.

Johnsen, K., Ryu, H.J., Grace, J.R. and Lim, C.J. Sorption-enhanced steam reforming of methane in a fluidized bed reactor with dolomite as $CO_2$-acceptor. Chemical Engineering Science 61 (2006): 1195 – 1202.

Keulen, A. N. J., Hegarty, M. E. S., Ross, J. R. H. and Oosterkamp, P. F. The development of platinum-zirconia catalysts for the $CO_2$ reforming of methane. Studies in Surface Science and Catalysis 107 (1997): 537-546.

Khatri, R. A. In situ infrared study of adsorbed species during catalytic oxidation and carbon dioxide adsorption. The Degree Doctor of Philosophy The Graduate Faculty of The University of Akron, 2005.

Kock, A. J. H. M., Bokx, P. K., Boellaard, E., Klop, W., Geus J. W. The formation of filamentous carbon on iron and nickel catalysts : II. Mechanism. Journal of Catalysis 96( 1985): 468-480.

Li, J. and Lu, G. Reaction performance of partial oxidation of methane over Ni/$SiO_2$ catalysts using monodisperse silica sol as supporting precursor. Applied Catalysis A: General 273 (2004): 163–170.

O'Connor, A. M. and Ross, J. R. H. The effect of $O_2$ addition on the carbon dioxide reforming of methane over Pt/$ZrO_2$ catalysts. Catalysis Today 46 (1998): 203-210.

Oliveira, E. L. G., Grande, C. A. and Rodrigues, A. E. $CO_2$ sorption on hydrotalcite and alkali-modified (K and Cs) hydrotalcites at high temperatures.Separation and Purification Technology 62 (2008): 137–147.

Promaros, E. Carbon dioxide reforming of methane under periodic operation. Master Degree Chemical Engineering Faculty of Engineering Chulalongkorn University, 2005.

Promaros, E., Assabumrungrat, S., Laosiripojana, N., Praserthdam, P., Tagawa, T., and Goto, S. Carbon dioxide reforming of methane under periodic operation. Korean Journal of Chemical Engineering 24 (2007): 44-50.

Promaros, E. Carbon dioxide reforming of methane under periodic operation. Master Degree Chemical Engineering Faculty of Engineering Chulalongkorn University, 2005.

Reijers, H. T. J., Valster-Schiermeier, S. E. A., Cobden, P. D. and Ruud W. van den Brink. Hydrotalcite as $CO_2$ Sorbent for Sorption-Enhanced Steam Reforming of Methane. Ind. Eng. Chem. Res. 45 (2006): 2522-2530.

Requies, J., Cabrero, M.A., Barrio, V.L., Guemez, M.B., Cambra, J.F., Arias, P.L., Perez-Alonso, F.J., Ojeda, M., Pena, M.A. and Fierro, J.L.G. Partial oxidation of methane to syngas over Ni/MgO and Ni/$La_2O_3$ catalysts. Applied Catalysis A: General 289(2005): 214-223.

Ruckenstein, E. and Yun Hang Hu. Methane partial oxidation over NiO/MgO solid solution catalysts. Applied Catalysis A: General 183 (1999): 85-92.

Takenaka, S., Umebayashi, H., Tanabe, E., Matsune, H. and Kishida, M. Specific performance of silica-coated Ni catalysts for the partial oxidation of methane to synthesis gas. Journal of Catalysis 245 (2007): 392–400.

Tang, S. B., Qiu, F. L. and Lu, S. J. Effect of supports on the carbon deposition of nickel catalysts for methane reforming with $CO_2$. Catalysis Today 24 (1995): 253-255.

Tomishige, K., Kanazawa, S., Suzuki, K., Asadullah, M., Sato, M., Ikushima, K. and Kunimori, K. Effective heat supply from combustion to reforming in methane reforming with $CO_2$ and $O_2$: comparison between Ni and Pt catalysts. Applied Catalysis A: General 223 (2002): 35-44.

Tsang, S. C., Claridge, J. B., and Green, M. L. H. Recent advances in the conversion of methane to synthesis gas. Catalysis Today 23 (1995): 3-15.

Vernon, P. D. F., Green, M. L. H., Cheetham, A. K. and Ashcroft, A. T. Partial oxidation of methane to synthesis gas, and carbon dioxide as an oxidising agent for methane conversion. Catalysis Today 13 (1992): 417-426.

Xiu, G., Li, P. and Rodrigues, A. E. Sorption-enhanced reaction process with reactive regeneration. Chemical Engineering Science 57 (2002): 3893 – 3908.

Zhang, T. and Amiridis, M. D. Hydrogen production via the direct cracking of methane over silica-supported nickel catalysts. Applied Catalysis A: General 167 (1998): 161-172.

# APPENDICES

# APPENDIX A

# CALCULATIONS FOR CATALYTIC PERFORMANCE

The gas sample from feed and product stream was analyzed by using a 1 mL gas sample injected into a gas chromatography in order to determine its composition. Concentration of each gas sample could be calculated from the calibration curve which was showed in Appendix B.

The sorption-enhanced carbon dioxide reforming and partial oxidation of biogas are operated under continuous feeds of methane, carbon dioxide and oxygen. The main reactions are $CH_4 + CO_2 \rightarrow 2CO + 2H_2$, $CH_4 + 1/2\,O_2 \rightarrow CO + 2H_2$, $CH_4 + 2O_2 \rightarrow CO_2 + 2H_2O$ and $CaO + CO_2 \rightarrow CaCO_3$. The total volumetric flow rate of the reactant feeds ($V_{inlet}$) was controlled to be 31.25 mL/min. Volumetric flow rate of product ($V_{outlet}$) can be measured from a bubble flow meter. Methane conversion was defined as molar flow rate of methane reacted at a particular period ($F_{CH_4 reacted}$), with respect to inlet molar flow rate of methane ($F_{CH_4 inlet}$)

$$
\begin{aligned}
CH_4\ Conversion &= \frac{(F_{CH_4,reacted})}{(F_{CH_4,inlet})} \times 100 \\
&= \frac{\left(F_{CH_4,inlet} - F_{CH_4,outlet}\right)}{(F_{CH_4,inlet})} \times 100 \\
&= \frac{\left(C_{CH_4,inlet} V_{inlet} - C_{CH_4,outlet} V_{outlet}\right)}{(C_{CH_4,inlet} V_{inlet})} \times 100 \qquad \text{(A.1)}
\end{aligned}
$$

Carbon dioxide and oxygen conversions also could be obtained in a similar method as calculation of methane conversion.

$$
CO_2\ Conversion = \frac{(C_{CO_2,inlet} V_{inlet} - C_{CO_2,outlet} V_{outlet})}{(C_{CO_2,inlet} V_{inlet})} \times 100 \qquad \text{(A.2)}
$$

$$O_2\ Conversion = \frac{(C_{O_2,inlet}V_{inlet} - C_{O_2,outlet}V_{outlet})}{(C_{O_2,inlet}V_{inlet})} \times 100 \qquad \text{(A.3)}$$

Hydrogen and carbon monoxide yield are calculated from molar flow rate of hydrogen respect to molar flow rate of methane inlet.

$$H_2\ Yield = \frac{1}{2} \times \frac{(C_{H_2,outlet}V_{outlet})}{(C_{CH_4,inlet}V_{outlet})} \times 100 \qquad \text{(A.4)}$$

# APPENDIX B

# CALIBRATION CURVES

This appendix shows the calibration curves for calculation of reactant and products composition in the sorption-enhanced carbon dioxide reforming and partial oxidation of biogas. The reactants are methane, oxygen and carbon dioxide. The products are synthesis gas, containing carbon monoxide and hydrogen.

The gas chromatography Shimadzu model 8A with a thermal conductivity detector (TCD) was used for analyzing the concentration of all reactants and products by using Molecular sieve 5A column and Porapak-Q column, respectively. Parameters used in for gas chromatography analyzing are illustrated in Table B.1. Operating conditions of gas chromatography for sorption-enhanced carbon dioxide reforming and partial oxidation of biogas are illustrated in Table B.2.

Mole of reagent in y-axis and area reported by gas chromatography in x-axis are exhibited in the curves. The calibration curves of methane, carbon dioxide, carbon monoxide, oxygen and hydrogen are shown in Figure B1, B2, B3, B4 and B5, respectively.

**Table B.1** Parameters used in Shimadzu model GC-8A

| Parameters | Condition (Shimadzu GC-8A) |
|---|---|
| Width | 5 |
| Slope | 50 |
| Drift | 0 |
| Min. area | 10 |
| T.DBL | 0 |
| Stop time | 20 |
| Atten | 7 |
| Speed | 2 |
| Method | 41 |
| Format | 1 |
| SPL.WT | 100 |
| IS.WT | 1 |

**Table B.2** Operating conditions of gas chromatography for the sorption-enhanced carbon dioxide reforming and partial oxidation of biogas

| Gas Chromatography | SHIMADZU GC 8A | |
|---|---|---|
| Detector | TCD | |
| Packed column | Molecular sieve 5A | Porapak-Q |
| - Column material | SUS | SUS |
| - Length (m) | 2 | - |
| - Outer diameter (mm) | 4 | - |
| - Inner diameter (mm) | 3 | - |
| - Mesh range | 60/80 | - |
| - Maximum temperature (K) | 623 | - |
| Carrier gas | Ultra high purity Ar | Ultra high purity Ar |
| Carrier gas flow rate (mL/min) | 40 | 40 |
| Injector temperature (K) | 373 | 373 |
| Detector temperature (K) | 373 | 373 |
| Column temperature | | |
| - initial (K) | 343 | 343 |
| - final (K) | 343 | 343 |
| Current (mA) | 70 | 70 |
| Analyzed gas | $CH_4$,$O_2$, $H_2$, CO | $CO_2$ |

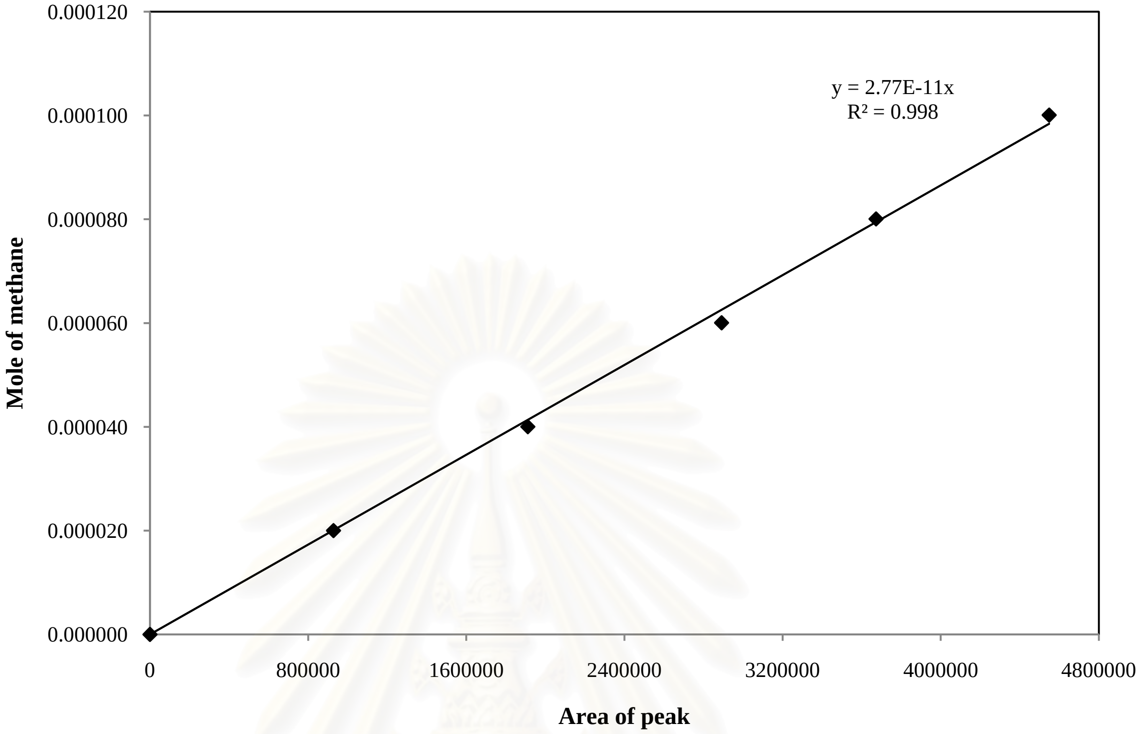

**Figure B.1** The calibration curve of methane

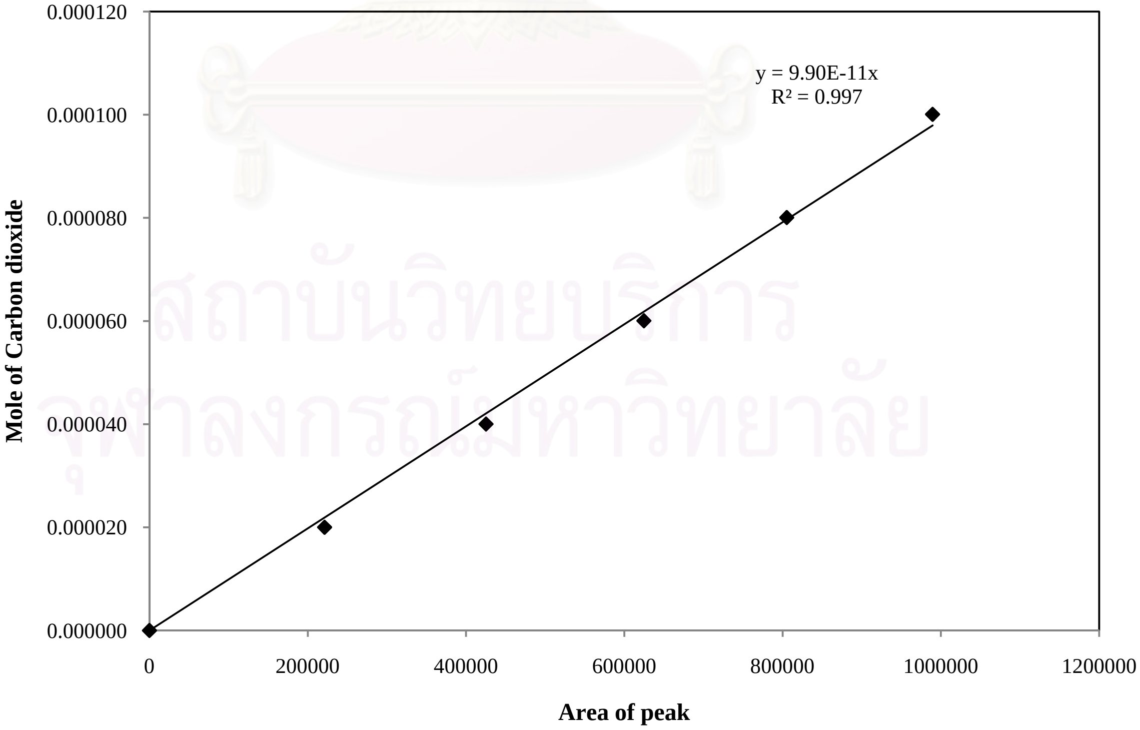

**Figure B.2** The calibration curve of carbon dioxide

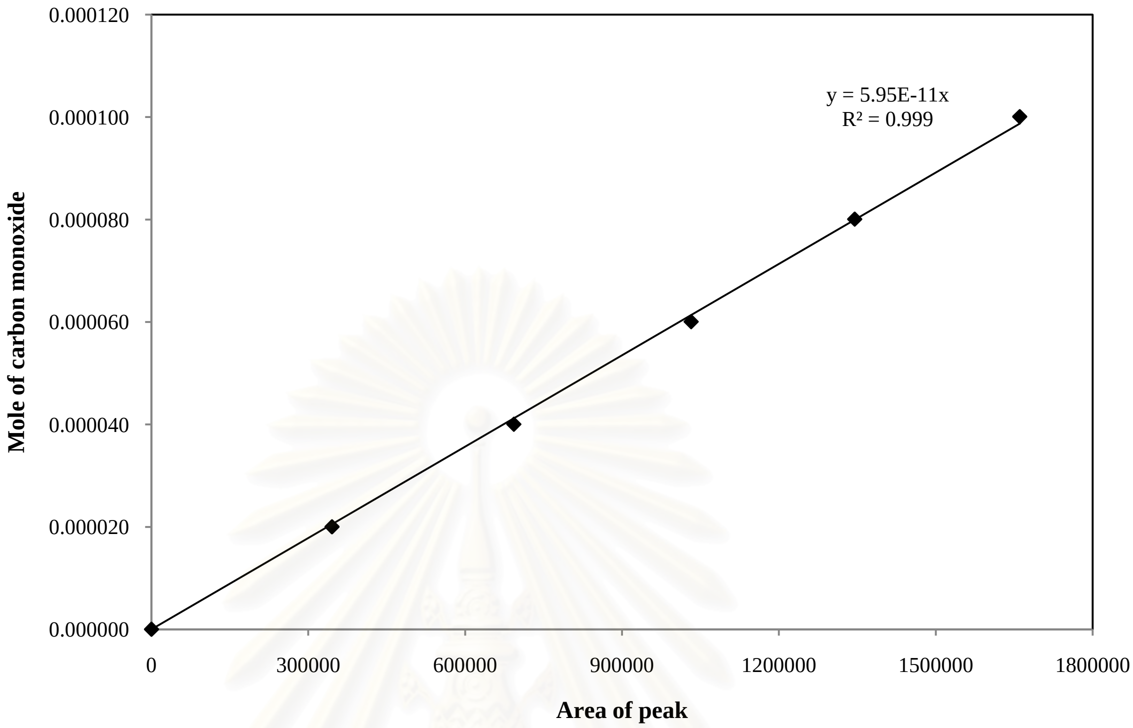

**Figure B.3** The calibration curve of carbon monoxide

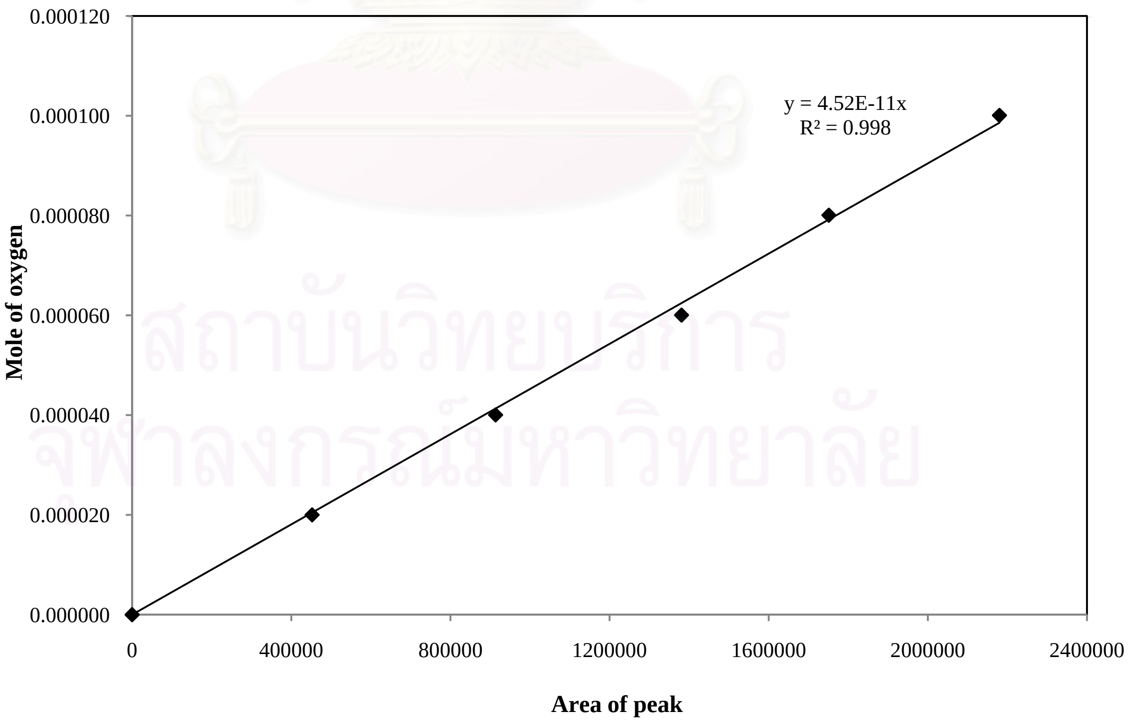

**Figure B.4** The calibration curve of oxygen

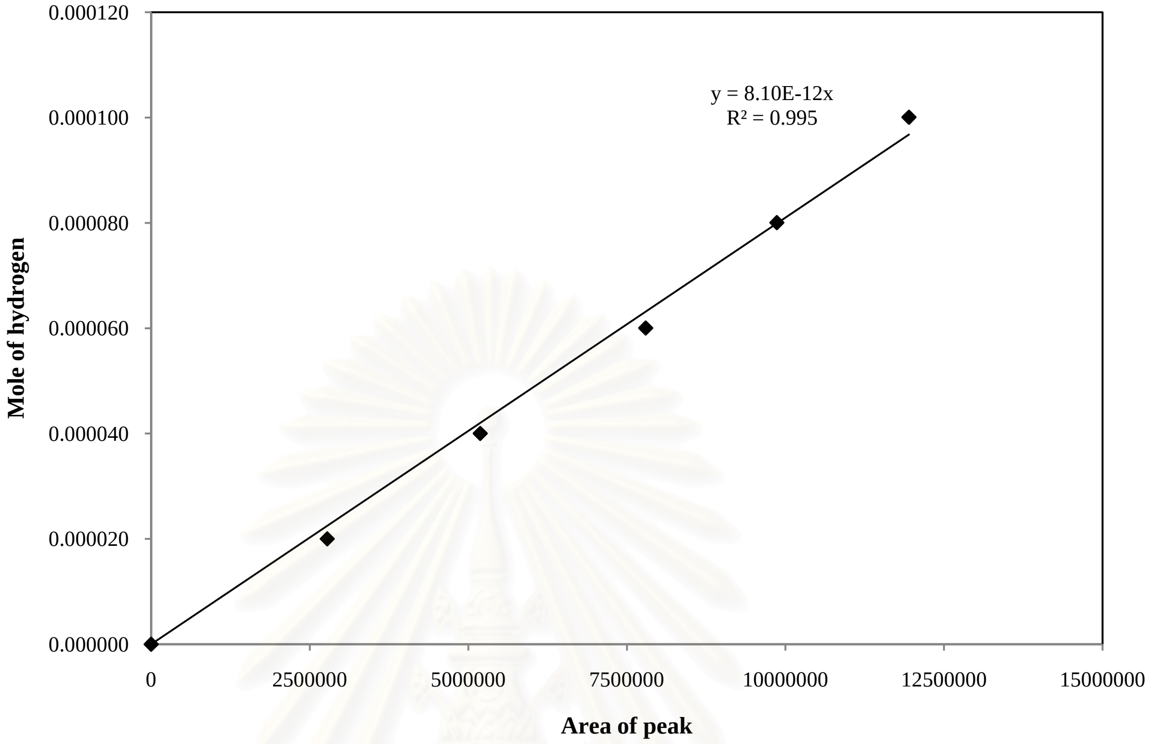

**Figure B.5** The calibration curve of hydrogen

# VITA

Miss Pornnipa Sonthisanga was born on February 26, 1985 in Bangkok, Thailand. She finished high school from secondary demonstration school of Suansunandha Rajabhat University, Bangkok in 2003, and received the bachelor’s degree in Chemical Technology from Faculty of Science, Chulalongkorn University in 2007. She continued her master’s degree study in Chemical Engineering from Faculty of Engineering, Chulalongkorn University in June, 2007.